# AN IN-VITRO INVESTIGATION OF GLUTATHIONE TRANSFERASES IN IDIOPATHIC PULMONARY FIBROSIS

by

Eileen Liberti

A Thesis
Submitted to the
Graduate Faculty
of
George Mason University
in Partial Fulfillment of
The Requirements for the Degree
of
Master of Science
Biology

Committee:

| | |
|---|---|
| _____ | Dr. Geraldine Grant, Thesis Director |
| _____ | Dr. Mikell Paige, Committee Member |
| _____ | Dr. Charles Madden, Committee Member |
| _____ | Dr. Iosif Vaisman, Acting Director, School of Systems Biology |
| _____ | Dr. Donna Fox, Associate Dean, Office of Student Affairs & Special Programs, College of Science |
| _____ | Dr. Peggy Agouris, Dean, College of Science |
| Date: _____ | Spring Semester 2018<br>George Mason University<br>Fairfax, VA |

# An In-vitro Investigation of Glutathione Transferases in Idiopathic Pulmonary Fibrosis

A Thesis submitted in partial fulfillment of the requirements for the degree of Master of Science at George Mason University

by

Eileen Liberti
Bachelor of Science
Saint Bonaventure University, 1984

Director: Geraldine Grant, Associate Professor, Assistant Chair
Department of Biology

Spring Semester 2018
George Mason University
Fairfax, VA

## DEDICATION

This is dedicated to my daughter Madeline and my husband Bill. Although I am last to finish a graduate degree, now we have a full set. Thank you for your support.

## ACKNOWLEDGEMENTS

Thank you to Dr. Geraldine Grant for all her support and guidance. Thank you to the Grant laboratory for camaraderie and encouragement. Sarah Bui was my lab teammate in our initial research, leading the way to a graduate degree. Luis Rodriguez provided invaluable support and guidance over the many months of this research. Sean Padden and Dr. Young-Ok graciously permitted use of the Tecan plate reader. Dr. Russell Hart of Arbor Assays provided vital technical assistance. Thank you to Dr. Paige and Dr. Madden for agreeing to be members of my committee. Thank you to Mrs. Virginia Colwell, Dr. Thomas Opfer, Dr. Michael Potter and all my colleagues at Paul VI Catholic High School for support and inspiration during my years of graduate school.

## TABLE OF CONTENTS

## LIST OF TABLES

## LIST OF FIGURES

## LIST OF ABBREVIATIONS AND SYMBOLS

Alpha-Smooth Muscle Actin (alpha-SMA) ..... ACTA2
Alveolar epithelial cell ..... AEC
Antioxidant response element ..... ARE
Apoptosis signal-regulating kinase 1 (MAP3K5) ..... ASK1
Bcl-associated x protein ..... BAX
B-cell lymphoma-2 ..... BCL2
B-cell lymphoma- long isoform ..... BCL2L1
c-Jun N-terminal Kinase ..... JNK
Collagen 1A1 ..... COL1A
Death Inducing Silencing Complex ..... DISC
Dulbecco Minimal Essential Media ..... DMEM
Ezatiostat hydrochloride ..... TLK199
Extracellular matrix ..... ECM
Fetal bovine serum ..... FBS
Glutathione ..... GSH
Glutathione disulfide ..... GSSG
Glutathione transferase ..... GST
Glutathione transferase Alpha ..... GSTA
Glutathione transferase Kappa ..... GSTK
Glutathione transferase Mu ..... GSTM
Glutathione transferase Pi (GST$\pi$) ..... GSTP
Human lung epithelial cells A549 (CCL-185) ..... A549
Human small airway epithelial cells ..... HSAEC
Hydrogen peroxide ..... $H_2O_2$
4-hydroxynonenal ..... HNE
Idiopathic pulmonary fibrosis ..... IPF
Kelch-like ECH-associated protein 1 ..... KEAP1
Kruppel-like factor 9 ..... KLF9
Membrane-associated proteins in eicosanoid and glutathione metabolism ..... MAPEG
Microsomal or MAPEG glutathione transferase ..... MGST
Mitogen-activated protein kinase ..... MAPK
NADPH oxidases ..... NOX
Nuclear factor-erythroid 2 related factor 2 ..... NRF2
Nuclear factor kappa-light-chain-enhancer of activated B cells ..... NF-$\varkappa$B
Oxidation-reduction ..... redox
Peroxiredoxin ..... PRDX

Phosphate buffered saline ..... PBS
Quantitative real time PCR ..... qPCR
Reactive nitrogen species ..... RNS
Reactive oxygen species ..... ROS
Tumor necrosis factor alpha ..... TNF-α
TNF receptor-associated factor 2 ..... TRAF2
Transforming growth factor-beta ..... TGF-β

## ABSTRACT

AN IN-VITRO INVESTIGATION OF GLUTATHIONE TRANSFERASES IN IDIOPATHIC PULMONARY FIBROSIS

Eileen Liberti, M.S.

George Mason University, 2018

Thesis Director: Dr. Geraldine Grant

Idiopathic pulmonary fibrosis (IPF) is a fatal interstitial disease of the lung. While pathogenic mechanisms are uncertain, IPF is described as a disease of dysregulated wound repair and is characterized by alveolar epithelial cell (AEC) death and excessive accumulation of activated fibroblasts. As part of the unchecked wound repair response, persistent IPF fibroblasts produce excessive extracellular matrix that destroys lung architecture and impairs gas exchange, eventually leading to death.

Lung tissue by its natural function experiences high oxidative stress. Additionally, IPF lung fibroblasts are known to excrete hydrogen peroxide. If IPF fibroblasts possess the ability to better metabolize and manage reactive oxygen species (ROS), it will contribute to their survival in the IPF lung. Management of this oxidative stress is mediated via superoxide dismutase, catalase and the highly polymorphic glutathione

transferases. This study examines the role that glutathione transferases (GSTs) and GST$\pi$ (GSTP) play in the management of oxidative stress and survival of the IPF fibroblasts.

Using an *in vitro* model of IPF this study was conducted using IPF and normal primary culture fibroblast cells (n = 3), human lung epithelial A549 cells and human small airway epithelial cells. Cells were challenged with $H_2O_2$ to simulate oxidative stress and survival was assessed with and without the GSTP inhibitor, TLK199. Gene expression was assessed by means of quantitative real time polymerase chain reaction (qPCR). GST enzymatic activity was evaluated using a fluorescent substrate reporter for total GST activity.

Increased survival in the presence of $H_2O_2$ was observed in IPF fibroblasts compared to normal fibroblasts. This increased survival correlated with both increased *GST* gene expression and increased GST enzyme activity in IPF fibroblasts. This is in contrast to normal fibroblast activity. Exposure to the GSTP inhibitor TLK199 in the presence of $H_2O_2$ decreased total GST enzyme activity and cell survival bringing IPF fibroblasts in line with normal fibroblasts. Our data also shows differential expression of *GST* isoforms in IPF fibroblasts with disease-specific upregulation of *GSTA4*, *GSTK1* and *GSTP1* in IPF fibroblasts in the presence of $H_2O_2$, demonstrating a more robust response to oxidative stress.

In this study we focus on the role played by GSTs as they relate to the metabolism of ROS in IPF. This differential metabolism may be instrumental in IPF fibroblast survival in the hostile environment of the IPF lung.

# INTRODUCTION

Idiopathic pulmonary fibrosis (IPF) is an age-related disease of the lung with undetermined pathogenesis. There are approximately 34,000 new cases diagnosed per year in the US with a median survival time of three years [1,2]. IPF is 100% fatal killing more than 26,000 people per year in the U.S., yet so little is known about its etiology [3]. In general, IPF is believed to be a disease of dysregulated wound repair. Whether this is driven by abnormal alveolar epithelial cells (AECs) or fibroblast response to injury, is unresolved. However, we do know that an abnormal response to an unknown trigger results in excessive recruitment and activation of fibroblasts resulting in excessive deposition of extracellular matrix, a.k.a. scar tissue. The buildup of excessive scar within the interstitial area of the lung results in dramatically reduced gaseous exchange, AEC death, loss of lung function and ultimately death [4].

There are currently two new treatments approved for IPF with conditional recommendations: Nintedanib and Pirfenidone [5]. Nintedanib is a tyrosine kinases inhibitor [6]. The exact mechanism of action of Pirfenidone (Esbriet®) is not known, however it is classified as an antifibrotic [7]. There are many drawbacks associated with these treatment, not least of which is the cost of more than $90,000 per year, but also include severe side effects and limited efficacy [5,8]. Therefore, there is no diminution in the urgent need to study the pathology of IPF and the cells that precipitate it to uncover

mechanisms that can be targeted for therapeutic intervention for this devastating, lethal disease.

Historically, multiple agents have been tested in search of effective therapy for IPF including anticoagulants. Although IPF presents with patterns reminiscent of usual interstitial pneumonia, patients showed poor response to anti-inflammatory agents. Even the newest agents, Nintedanib and Pirfenidone, only merit the same recommendation status as antacid therapy [5]. IPF remains a paradox. One of the unresolved issues is the presence of ROS; whether representing the insult or a symptom of the injury, the pleiotropic effects of ROS are inevitable.

Lung tissues, by nature, are exposed to elevated oxygen levels, exogenous oxidants and pollution. Antioxidants and antioxidant enzymes have evolved to cope and defend against this stress. The importance of antioxidants to counteract oxidation is demonstrated by the development of multiple, overlapping antioxidant systems. An imbalance in oxidant-antioxidant defense leads to a variety of diseases associated with aging and fibrosis including IPF [9,10]. IPF research continues to explore the roles of several antioxidant systems including glutathione (GSH), catalase, superoxide dismutase and nuclear factor erythroid-2 [10]. A diminished concentration of GSH has been reported in the pulmonary lavage fluid of individuals with IPF reflecting reduced cellular production of GSH. It follows that a reduced ability to cope with ROS could be related to an alteration in GSH synthesis [11]. N–acetylcysteine, a precursor to GSH, has undergone clinical trials for the treatment of IPF. After some initial positive data, no significant differences between treatment and non-treatment groups were found. For this reason the

American Thoracic Society Clinical Guidelines are reticent to recommend the use of N-acetylcysteine as a monotherapy and strongly discourages the use of the combination prednisone/azathioprine/N–acetylcysteine [5]. ROS remain an important but unresolved factor in the development of IPF and the environment of the IPF lung.

IPF pathogenesis is associated with wound healing gone awry. Normal wound-healing involves multiple cells and resolves with return to homeostasis for each cell type. Injuries typically damage epithelial cells followed by recruitment of a variety of cell types to the area for repair processes. IPF pathogenesis centers on the interplay between AECs and fibroblasts resulting in imbalance of cell types. While the specific nature of injury may vary, increases in AEC death and phenotypic changes to the surviving AEC are well documented [12–15]. Cell death may be signaled via intrinsic or extrinsic apoptotic pathways and both pathways are active in IPF. AECs in the IPF lung display increases of pro-apoptotic BAX (Bcl-associated x protein) but low levels of anti-apoptotic BCL2 (B-cell lymphoma-2) and BCL2L1 (B-cell lymphoma - long isoform) that contribute to susceptibility to cell death through the intrinsic pathway [16]. The extrinsic pathway signals apoptosis through activation of cell surface receptors including FAS by its ligand, FASL. AEC in the lungs of IPF patients upregulate *FAS* and are thus more susceptible to extrinsic apoptosis [14].

IPF lung tissue includes an overabundance of fibroblasts that are resistant to apoptosis [13]. Resident fibroblasts are joined by circulating fibrocytes and epithelial cells that transition to mesenchymal phenotypes [17]. These cells differentiate into activated myofibroblasts [18,19]. After tissue damage initiates migration and activation to

myofibroblast, production of actin-associated cell-cell and cell-matrix connections as well as extracellular matrix (ECM) synthesis commence [18]. Key markers for identification of activated myofibroblasts are high expression of alpha-smooth muscle actin and type-I collagen [20]. In IPF fibroblasts demonstrate resistant apoptotic patterns as opposed to the increased cell death in AEC. IPF fibroblasts downregulate pro-apoptotic *BAX* and upregulate anti-apoptotic *BCL2* and *BCL2L1* contributing to resistance to apoptosis [16]. Myofibroblasts in IPF also increase surface FASL and provoke extrinsic apoptosis in AEC [14].

The IPF lung environment impacts both apoptotic susceptible AECs and apoptotic resistant fibroblasts. Lung tissues are subject to the highest levels of oxygen and are vulnerable to oxidative stress. Oxidative stress includes molecular, cellular and tissue damage due to imbalance of ROS and antioxidants [21]. Reactive oxidants may come from endogenous or exogenous sources including drugs and xenobiotics [21]. Additionally, IPF fibroblasts release extracellular $H_2O_2$ that induces epithelial cell death [22]. ROS are generated by the mitochondrial electron transport chain and enzymes such as cytochrome P450, cyclooxygenases, lipoxygenases and NADPH oxidases [23]. The NADPH oxidases (NOX), in particular NOX4, appear to make a major contribution to ROS production promoting fibrosis including IPF [24].

ROS are linked to production of growth factors and cytokines as well as activation of latent cytokines (Figure 1). In IPF both feed-back and feed-forward systems link ROS and cytokine activity [24]. Transforming growth factor-β (TGF-β) is established as a key mediator of fibrosis and overexpressed in IPF fibroblasts [23]. TGF-β1 promotes

ROS production through expression of *NOX4* while the resultant ROS increase production and activation of TGF-β [24]. The effects of TGF-β extend far beyond interaction with NOX4.

Additionally, TGF-β increases overall ROS levels in the IPF lung by down-regulation of multiple antioxidant enzymes including glutaredoxin, catalase, superoxide dismutase and glutathione peroxidase [25]. This down-regulation impairs detoxification of ROS including superoxide dismutase conversion of superoxide radicals into $H_2O_2$ that catalase may decompose into oxygen and water [9]. Decreased expression of several antioxidants impedes ROS detoxification and creates higher oxidant to antioxidant ratios. High ROS levels feed-forward towards fibrotic mechanisms and feed-backward to activation of TGF-β [23]. The antioxidant systems unaffected by TGF-β must bear a greater burden for ROS management and become potentially crucial factors in the IPF lung.

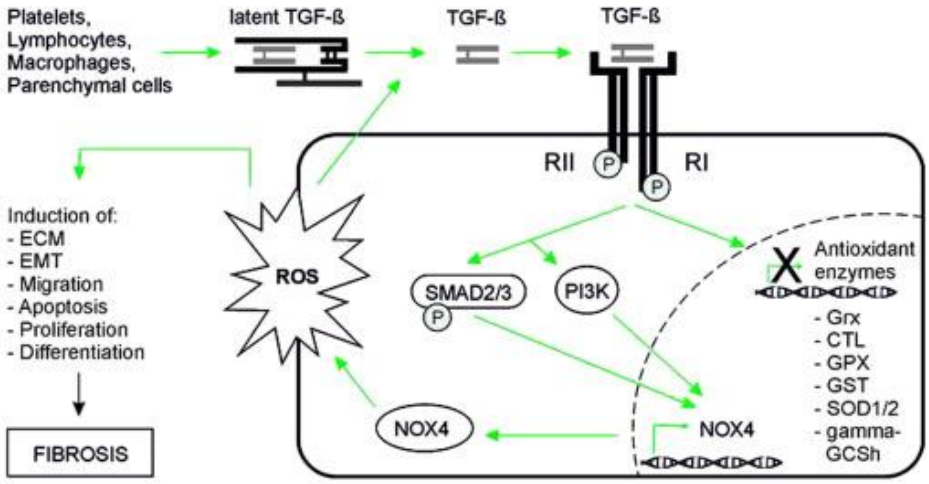


**Figure 1 ROS and TGFβ mediation of fibrosis**
**ROS activates latent TGFβ and binding to its receptor. Signaling pathways are initiated to induce expression of *NOX4* and subsequent increases in ROS. TGFβ also down regulates expression of antioxidant enzymes leading to an increase in the NOX4/antioxidant ratio and ROS imbalance. Excessive ROS promotes fibrotic processes.** [23]

## Glutathione Antioxidant Defense

Glutathione (GSH) is a tripeptide with multiple functions including antioxidant defense and cell signaling. Found in virtually all cells, it is the most abundant and important low molecular weight thiol with concentrations of 1–2 mM in most cells [26]. GSH is synthesized from glutamate, glycine and cysteine retaining its critical thiol (-SH) group that generates the antioxidant activity [27]. The structure of GSH, γ-L-glutamyl-L-cysteinylglycine (Figure 2), has unusual resistance to peptidases due to the γ-glutamyl bond [28]. As a major intracellular antioxidant, GSH provides a wide spectrum of activity and protective effects. Most important reactions of GSH involve the reactive sulfhydryl as a nucleophile in its ionized form [28].

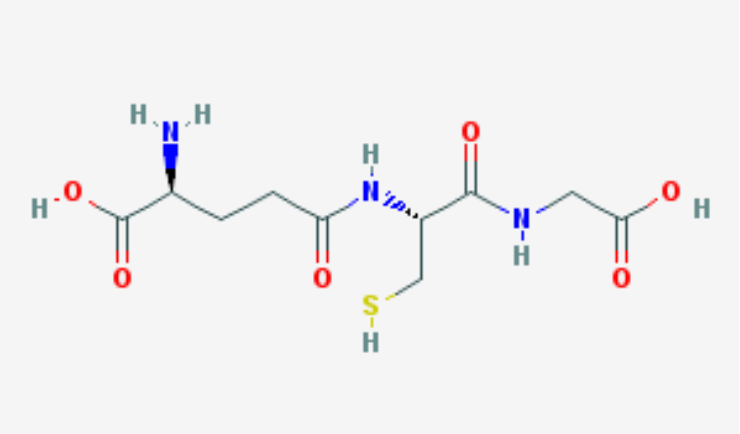

**Figure 2 Glutathione structure**
**National Center for Biotechnology Information. PubChem Compound Database; CID=124886, https://pubchem.ncbi.nlm.nih.gov/compound/124886 (accessed Nov. 10, 2017).**

GSH has a broad range of activity. GSH acts as an antioxidant, directly as a free radical scavenger and indirectly as a detoxifying agent through conjugation to toxic compounds rendering them more suitable for excretion. In addition, GSH participates in the uptake of amino acids and synthesis of leukotrienes. GSH is also involved in the formation and maintenance of disulfide bonds in proteins. Low GSH levels within the endoplasmic reticulum interferes with disulfide bond formation and isomerization [29]. In the liver GSH is essential for detoxification of lipophilic toxins during biotransformation producing bile. GSH participates in production of red and white blood cells as well as immune processes [27]. In addition to direct detoxification of ROS, GSH aids metabolism of toxic products of oxidation. GSH functions as a buffering system in the redox pathway and regulates cellular metabolism including cell proliferation, signal transduction and

gene expression [30]. GSH and management of ROS is of specific interest in the IPF lung environment.

## Redox Homeostasis

As both a reducing agent and antioxidant, GSH directly contributes to redox homeostasis. Imbalance in the GSH redox system is a longstanding suspect in the IPF lung [11]. ROS have the potential to damage DNA, proteins, and membrane lipids in addition to peroxidation of lipoproteins. While some result from exogenous oxidants, ROS are an inherent product of aerobic metabolism. Reactive nitrogen species (RNS) inhibit DNA and protein synthesis as well as inactivate respiratory chain complexes. Both RNS and ROS are reduced and inactivated through formation of a disulfur bond between two GSH molecules (Figure 3) producing glutathione disulfide (GSSG). This process is catalyzed by glutathione peroxidase. Free GSH is then recovered by the action of glutathione reductase [31].

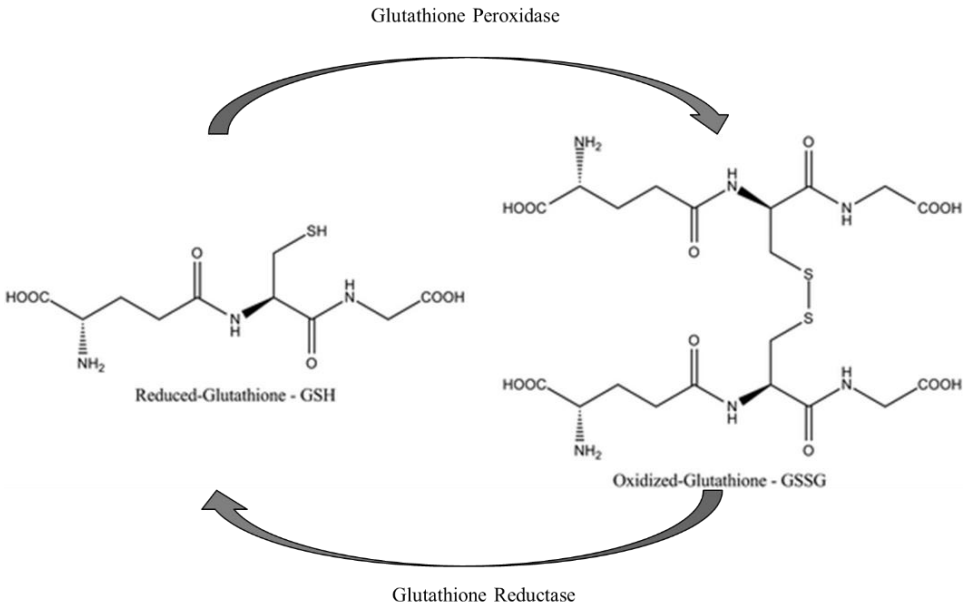


**Figure 3 GSH – GSSG cycle**
**The oxidation reduction cycle of GSH participates in redox homeostasis.**

GSH was originally associated with drug detoxification. GSH affords protection from ROS including reactive nitrogen species and dietary oxidants. Carcinogens may be conjugated with GSH, reducing their toxicity and providing a path for excretion [30]. The focus of GSH detoxification is directed in part by the specific enzyme catalyzing the reaction of GSH with its target substrate [32]. GSTs are conventionally classified as phase II enzymes in drug metabolism, although they deliver broad protection for the cell including inactivation of endogenous metabolites of oxidative stress. Antioxidant functions are critical in the oxidative environment of the IPF lung.

## Drug Metabolism

GSH and GSTs are major participants in detoxification of detrimental substances and processing of drug metabolites [33]. Drug metabolism is the enzymatic breakdown of harmful compounds of exogenous origin, xenobiotics, as well as endogenous processes. This form of biotransformation is conserved throughout in all major groups of organisms.

Traditionally, drug metabolism includes three phases. Phase I drug metabolism reactions include oxidations, reductions and hydrolytic activities that create functional groups increasing water solubility. The most common example of phase I reactions are the hydroxylation reactions of the cytochrome P-450 protein family [34]. These functional groups may also provide a point of attachment for endogenous moieties during phase II should such anchoring sites not be contained in the original xenobiotic structure.

Phase II reactions are synthesis reactions, predominantly conjugations, which generally reduce toxicity and increase solubility. While exceptions occur, conjugation inactivates the xenobiotic substrate and expedites excretion [35]. The resultant conjugates continue into phase III metabolism encompassing the export of these metabolites from the cell (Figure 4). As one might expect, a metabolic and exocytotic process is not a strict sequential progression; there is great variability in drug metabolism [35,36].

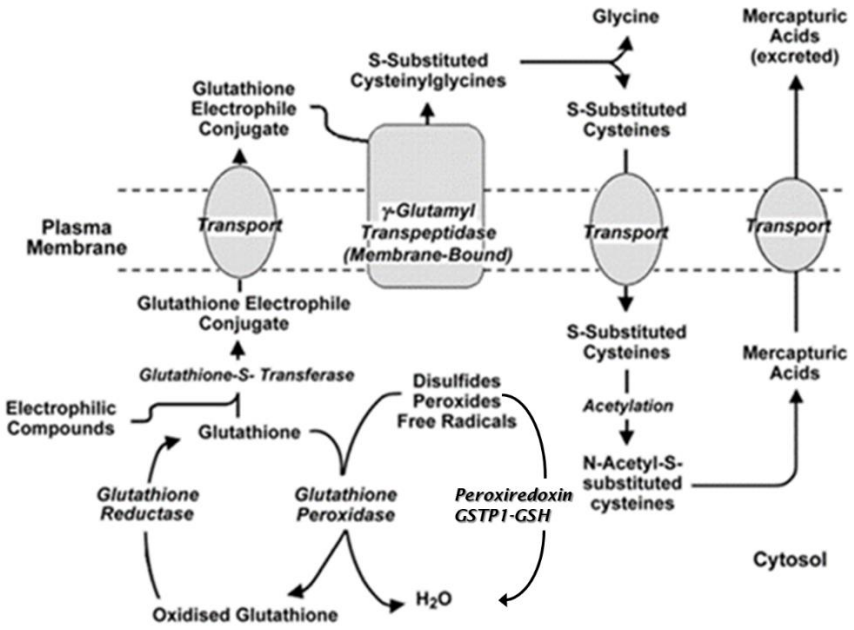


**Figure 4 The GSH Pathway and Drug Metabolism**
**GSH metabolizes ROS through the action of glutathione peroxidase. Oxidized GSSG is reduced to recover free GSH. GSH conjugates with electrophilic moieties via the action of GSTs. Glutathione conjugates are transported and eventually processed through the mercapturic acid pathway.**
[31]

## Glutathione transferases

As in any partnership, disruption of balance and activity leading to fibrosis may result from low availability or malfunction of any collaborating protective molecule. Glutathione transferases (GSTs), previously known as glutathione S-transferases, facilitate the conjugation of GSH with the electrophilic center of an acceptor molecule of endogenous or exogenous origin [28]. *GSTs* encompass three superfamilies of genes, the canonical cytoplasmic *GST*s, the *Kappa*-class, and *MAPEG* (membrane-associated

proteins in eicosanoid and glutathione metabolism), also known as microsomal (*MGST*s). The members of the MAPEG family are integral membrane homotrimers produced by three genes in humans, *MGST1*, *MGST2*, and *MGST3*. MAPEG enzymes protect membranes from lipid hydroperoxides. Kappa-class GSTs (GSTK) are found in mitochondria and peroxisomes. The cytosolic GSTs comprise several classes and tend to form homodimers or heterodimers within their class [28,35].

The cytoplasmic GSTs are the best understood GSTs. The Alpha (GSTA), Mu (GSTM) and Pi (GSTP) classes are predominant in mammals and are the most investigated classes. Generally, these classes share the prototypical GST structure but differ at the subunit interface and active site (Figure 5). The subunit interface varies between classes preventing formation of heterodimers across classes [28]. The active site contains two binding sites, the G-site for GSH and the H-site for hydrophobic substrate binding [37]. GSTA and GSTM both have comparatively hydrophobic electrophile binding sites within the active site. However, structural differences result in a mobile C-terminal α-helix covering the GSTA active site while the GSTM active site is only partially occluded by a "Mu loop". GSTP enzymes have an open active site conformation with both hydrophilic and hydrophobic binding site characteristics [28].

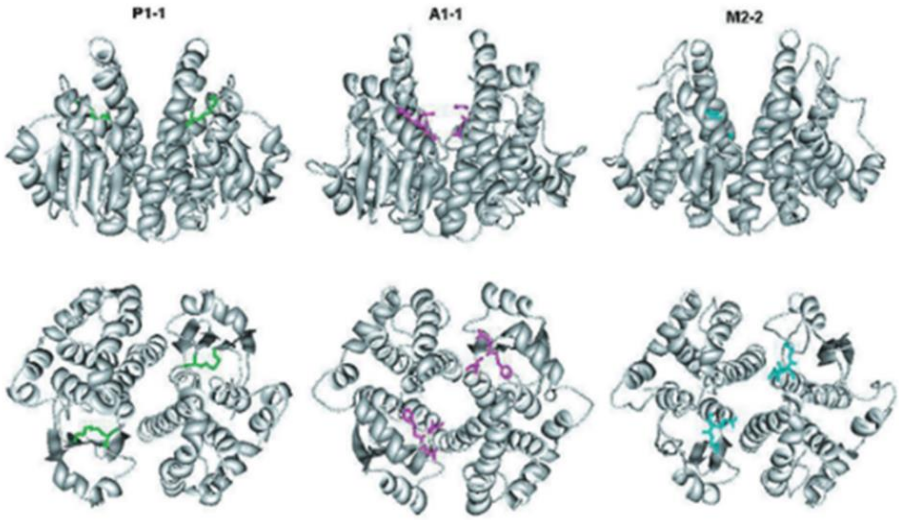


**Figure 5 GSTA, GSTM and GSTP structure**
**Ribbon structures of GSTP1-1, GSTA1-1 and GSTM2-2 with the GSH molecule in color at the active site [38]**

The remaining classes are less prevalent in humans. Sigma-class *GST*s are more highly expressed in invertebrates but specialize in prostaglandin synthesis and isomerization in mammals. Theta- and Zeta-classes share a key structural difference in the active site with tyrosine replaced by a serine for activation of GSH. The Omega-class utilizes an active-site cysteine. The Omega-class GSTs resemble glutaredoxins in this structure and in function, with minimal activity towards customary GST substrates. In human lung the most abundant GST is GSTP followed by GSTA and GSTM, respectively. Only minor expression of the remaining classes is normally found in lung tissue [28].

Both cytosolic and mitochondrial GSTs facilitate the nucleophilic attack of reduced GSH on the electrophilic center of nonpolar compounds. This is accomplished

by reducing the pKa of GSH from 9.0 to less than 7 within the active-site of the enzyme. Both families also reduce organic hydroperoxides but are inactive with hydrogen peroxide as a substrate [28].

Another indirect antioxidant mechanism for GSH-GST is through partnership with Peroxiredoxin (PRDX). PRDXs are an extensive family of peroxidases that reduce peroxides like $H_2O_2$, lipid peroxide, or peroxynitrite via a conserved cysteine residue [39]. While there are multiple enzymes for peroxide decomposition such as catalase and glutathione peroxidase, several are down-regulated in IPF by TGF-β [25,40]. PRDX6 is the only mammalian PRDX and requires GSTP to deliver GSH and facilitate formation of GSSG [39,41].

Imbalance in oxidation-reduction (redox) status or oxidative stress is of specific interest in IPF [9–11,42]. IPF fibroblasts export $H_2O_2$ [22] and display high levels of TGF-β and NOX4 that increase ROS levels while decreasing expression of multiple antioxidants in the IPF environment [24,40]. The result is oxidative damage in IPF lungs. The GST-GSH antioxidant system provides another protective process through S-glutathionylation, GSH conjugation to reactive cysteines within proteins. S-glutathionylation is reversible and provides protection for the reactive cysteine and protein structure from oxidative damage. The reversible nature of S-glutathionylation forms an avenue linking redox status to cell signaling pathways [43].

## Cell Signaling

Clearly, the ability of a cell to sense redox status and respond appropriately is essential for maintenance of homeostasis [13]. GSTs affect metabolic pathways and gene regulation in several ways. Oxidative stress promotes reversible S-glutathionylation of proteins with reactive cysteines. Thus, the S-glutathionylation and de-glutathionylation process functions as a regulatory, post-translational modification generating target specific changes to protein structure similar to phosphorylation or acetylation [43].

GSTs demonstrate regulatory functions through direct protein-protein interaction. GSTP inhibits c-Jun N-terminal Kinase (JNK) without facilitating conjugation. JNK is a mitogen-activated protein kinase (MAPK) involved in stress response, proliferation, apoptosis and inflammation [44]. GSTP may regulate basal levels of JNK by routine interaction with a modest reservoir of JNK then dissociate due to increased ROS. Dissociation releases a burst of JNK promoting activation of c-JUN. Thus, tumor upregulation of GSTP would increase sequestration of JNK and repress apoptotic signaling [45]. Most human tumor cell lines overexpress GSTP [44]. This chain represents one path imparting resistance to drug induced apoptosis.

Metabolic regulation through S-glutathionylation is demonstrated by involvement in the extrinsic apoptotic pathway (Figure 6) [46]. After initiation of the caspase cascade, cysteine 294 of the FAS death domain becomes S-glutathionylated which signals the formation of the “Death Inducing Silencing Complex” (DISC) [47].

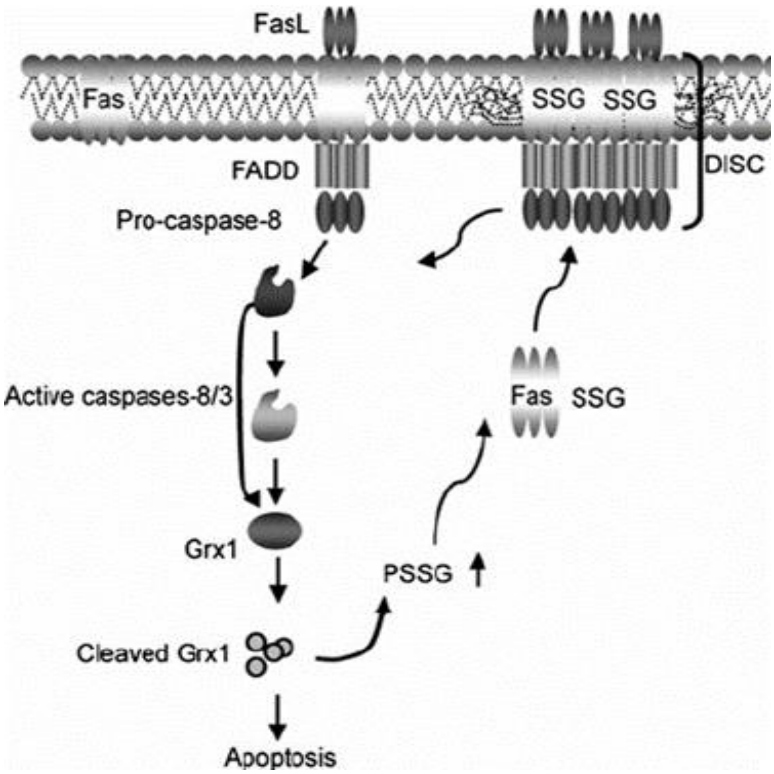


**Figure 6 FAS death domain S-glutathionylation**
**S-glutathionylation participates in feed forward amplification of apoptosis through promotion of FAS binding and formation of DISC [43].**

Regulation of apoptotic pathways is of particular interest in IPF as epithelial cells in IPF patients are quite susceptible to cell death whereas activated myofibroblasts in IPF are highly resistant to apoptosis [48]. The FAS death receptor is highly expressed on lung epithelial cells in IPF and participates in signaling apoptosis in AEC [49]. IPF fibroblasts produce FAS ligand that may potentiate AEC cell death yet are resistant to FAS induced death themselves [43].

It has been established that an alteration in oxidant/antioxidant homeostasis contributes to the pathogenesis of lung fibrosis including observed low levels of

extracellular GSH in IPF lungs [10,11]. Strategies to increase production of GSH have been utilized, such as N-acetylcysteine treatments but have had mixed responses and discouraging results. If production of GSH is not an efficacious therapeutic target, then other related molecular targets should be considered [10]. One such target is the GSTs.

Regulation of GST activity and *GST* gene expression contributes to redox homeostasis. *GST* promoters contain antioxidant response elements (AREs) for transcriptional activation by Nuclear factor-erythroid 2 related factor 2 (NRF2) triggered by oxidative stress [50]. Without oxidative stress, NRF2 is sequestered in the cytosol by Kelch-like ECH-associated protein 1 (KEAP1) [23]. ROS leads to KEAP1 dissociation and release of NRF2 to move into the nucleus, bind at AREs and promote expression of antioxidants [50]. The NRF2 antioxidant regulation pathway diminishes bleomycin-induced lung fibrosis [51].

## GST Inhibitors

GSTs and S-glutathionylation connect oxidative stress in IPF to signaling pathways and apoptosis [43]. The NRF2-ARE pathway connects expression of antioxidants, including *GST,* to mitigation of lung fibrosis [51]. Although therapeutic targeting of GSH production provides little benefit [5], evaluating GST enzyme function is an alternative avenue of investigation. GST inhibitors were originally developed as adjuncts to existing cancer therapies, but their contribution likely depends on the drug, cell type, and transporters involved [38]. Modifications to glycine and cysteine residues in the GSH backbone yield inhibitors with potential while the γ-glutamyl residue must remain

unmodified to allow binding [44]. TLK199 is a diester analog of GSH (Figure 7) with α-phenyl glycine and benzyl conjugated cysteine [38]. Esterification increases cellular uptake of TLK199. Intracellular de-esterification produces the active form, TLK117, that binds to the G-site of GSTP1-1 [52].

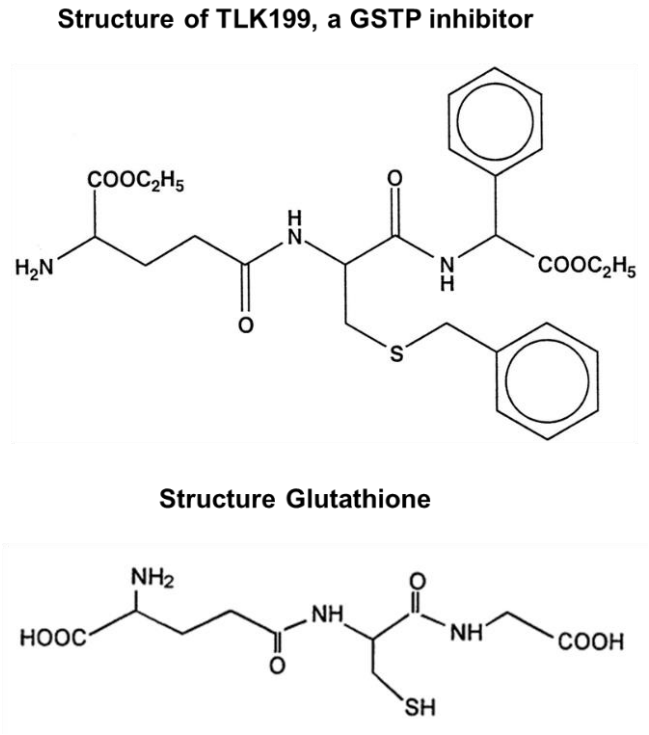


**Figure 7 Comparison of TLK199 Structure and Glutathione Structure [52]**

## GSTP Inhibitors and IPF

*GSTP* is highly expressed in lung tissue, particularly the AEC [53]. Based on the connection between IPF and oxidative stress, the role of GSTP in management of ROS is pertinent. McMillan, et al., reported an attenuation of the fibrotic response, including

both production of collagen and α-smooth muscle actin in GSTP -/- mice. This strongly suggested that interfering with GSTP activity by a repressor, TLK117, could produce a similar favorable response. The use of the GSTP inhibitor TLK117 attenuated epithelial cell death and lung remodeling in induced IPF models using bleomycin- and adenovirus vector AdTGFβ-induction [54]. While McMillan demonstrated reduced epithelial cell death, the response of fibroblasts to GSTP inhibitor is not assessed. Our study investigates the response of human cells, specifically normal fibroblast and IPF myofibroblast, to GSTP inhibition. TLK199, the prodrug of TLK117, is readily available and has completed phase I and II clinical trials for myelodysplastic syndrome [55]. The TLK199 prodrug is hydrolyzed after entering the cell to a diacid form that binds GSTP1-1 [56].

This study investigates oxidative stress in Idiopathic Pulmonary Fibrosis and the role of Glutathione Transferase in redox regulation.

- Aim 1: Examine the expression of glutathione transferases in IPF and normal fibroblasts
- Aim 2: Examine the effect of oxidative stress on expression of glutathione transferases and their potential role in cell survival for IPF and normal fibroblasts.
- Aim 3: Examine the potential protective/pro-survival role of glutathione transferases in IPF by modulating the activity of GSTP1 during oxidative stress.

# MATERIALS AND METHODS

## Materials

All chemicals and supplies were purchased from ThermoFisher Scientific (Pittsburgh, PA) unless specified. Ezatiostat hydrochloride (TLK199) was purchased from ApexBio (Houston, TX).

Human lung epithelial cells A549 (CCL-185) were obtained from the American Type Culture Collection (ATCC, Manassas, VA). Human small airway epithelial cells (HSAEC) were obtained from the laboratory of Dr. Serguei Popov (GMU, Manassas, VA). IPF and normal cells used in this study were previously isolated and frozen in 10% Dimethyl Sulfoxide (DMSO).

### *Donor Consent and Internal Review Board Approval*

The IPF cell lines were isolated from IPF lung tissue obtained through Inova Fairfax Hospital (VA). Normal fibroblast cell lines were developed from control lungs acquired via the Washington Regional Transplant Community (WRTC). Appropriate consent was obtained for each patient and donor lung by Inova Fairfax hospital and the WRTC. This process was approved by the Inova Fairfax Hospital Internal Review Board

(IRB #06.083) and the George Mason University Human Subject Review Board (Exemption #5022).

## Methods

*Primary fibroblast isolation and culture*

The primary fibroblasts used in this study were originally isolated from human lungs procured in the operating room within minutes of the removal of the pulmonary tissue. Consistent dissection was performed by orienting the lungs from apex to base. Isolation was performed through differential binding [57]. After dissection of lung tissue into 1-2 $mm^2$ pieces enzymatic digestion was performed in 0.4% collagenase P (Roche, Indianapolis, IN) complete media (Dulbecco Minimal Essential Media (DMEM) containing 10% fetal bovine serum (FBS), penicillin (100 I.U/ml), streptomycin (100 MCH/ml), amphotericin B (0.25 M.C.G./ml P/S/A) and 0.1% DNase1, at 37ºC and 5% $CO_2$ for 2 hours. Sterile filtration (40, 100 µ nylon mesh) was followed by centrifugation at 1000g for 5 min and resuspension in complete media for seeding onto non-tissue culture plastic for 10 minutes at 37ºC and 5% $CO_2$. The supernatant containing unattached cells was transferred to tissue culture treated plastic at 37ºC and 5% $CO_2$ for 45 minutes allowing attachment of the fibroblast population. Washing with phosphate buffered saline (PBS) removed unattached cells

Fibroblasts were cultured in vitro ≤ 80% confluence and maintained within a 10-passage range in a Hyclone Dulbecco's Modified Eagle medium (DMEM, Invitrogen) supplemented with 10% Fetal Bovine Serum (FBS, Atlanta).

*Pretreatment of cells*

All cells were uniformly prepared for each experiment. Cells grown to ≤ 80% confluence were serum-starved overnight. Cells were trypsinized (0.25% Trypsin-EDTA Gibco) and seeded at a concentration of 100,000 cells per well in a tissue culture treated six-well dish in DMEM with 10% FBS for RNA extraction. Cells for toxicity and survival assays were seeded at a concentration of 5000 cells per well in tissue culture treated 96 well plates in DMEM with 10% FBS. After overnight attachment of 16-24 hours, cells were exposed to experimental conditions.

*Cell Survival Analysis*

After standard cell pretreatment and seeding into 96 well, tissue culture treated plates, initial toxicity tests were performed using acid phosphatase substrate 4-Nitrophenyl phosphate bis (tris) salt (Sigma-Aldrich) colorimetric analysis and read at 405 nm using the BioTek ELx800 plate reader. Appropriate hydrogen peroxide solution (Sigma-Aldrich #216763 with inhibitor 30wt. % in $H_2O_2$, ACS reagent) concentrations were identified for high ROS stress conditions at 1 mM and nonlethal stimulatory conditions at 200 μM. Toxicity testing of TLK199 confirms 50 μM TLK199 alone does not significantly affect cell viability.

*Experimental treatment of cells*

To allow sufficient time for the inhibitor to enter the cells and take effect, the inhibitor groups were pre-treated with 50 μM TKL199 for 2 hours followed by overnight exposure to 200 μM $H_2O_2$ in DMEM. The inhibitor treatment group was compared to

DMEM media control and 200 μM $H_2O_2$ in DMEM. After 24 hours, cells were assayed for viability or flash frozen in liquid nitrogen and stored at -80 °C for RNA extraction.

Cell survival under media control and treatment conditions was performed in 96 well, tissue culture treated plates and assessed using CellTiter-Glo® Luminescent Cell Viability Assay (Promega, Madison, WI) that generates a luminescent signal proportional to the amount of ATP present and read with the Biotek FLx800 plate reader.

*Total RNA Extraction*

Total RNA was extracted using the RNeasy® Kit (Qiagen) after 24 hours from media control, exposure to non-toxic 200 μM $H_2O_2$ without inhibitor and with 2-hour 50 μM TLK199 pretreatment prior to 200 μM $H_2O_2$. RNA was quantified using a Nanodrop™ spectrophotometer (Nanodrop™ 3.0.0, Agilent Technologies) and stored at -80° C.

*Real-Time Polymerase Chain Reaction*

Gene expression was assessed by quantitative real time PCR (qPCR). Total RNA (1μg) was reverse transcribed to cDNA using the Verso cDNA synthesis kit. qPCR was performed using the Quantifast SYBR green PCR kit (Qiagen). Gene expressions were normalized to 18S gene expression using the Comparative Ct 2-(delta)(delta)Ct method and converted to fold change compared to media control values [58].

Expression scores are derived from the Comparative Ct 2-(delta)(delta)Ct method and enable representation and comparison of baseline media qPCR values (Appendix B). As with fold change, expression scores are relative values within each gene but allow comparison of gene expression in control conditions. GST isoforms are not necessarily

uniformly regulated and likely differ by cell type [32,59]. Inhibition of GSTP1 may result in differential upregulation of other GST isoforms.

qPCR gene expression analysis utilized primers for alpha-Smooth Muscle Actin (alpha-SMA) (*ACTA2*), Collagen 1A1 (*COL1A*) (Integrated DNA Technologies). *ACTA2* and *COL1A1* expression serve as markers for activation level of the cell lines. Primers for a series of GST enzymes are also used for qPCR: *GSTA1, GSTA4, GSTK1, GSTM2, GSTM3, GSTO1, GSTP1, GSTT2,* and *GSTZ1* (Integrated DNA Technologies). The sequence for all primers used are found in Table 1.

**Table 1 Primer Sequences for qPCR**

| | |
|---|---|
| *18S* Forward | 5'- GAT GGG CGG GGA AAA TAG-3' |
| *18S* Reverse | 5'- GCG TGG ATT CTG CAT AAT GGT-3' |
| *ACTA2* Forward | 5'- GCT GGG ACA TTG AAA GTC TCA-3' |
| *ACTA2* Reverse | 5'- GTG TTG CCC CTG AAG AGC AT-3' |
| *COL 1A1* Forward | 5'- CAG ATC ACG TCA TCG CAC AAC-3' |
| *COL 1A1* Reverse | 5'- GTC GAG GGC CAA GAC GAA G-3' |
| *GSTA1* Forward | 5'- GTG CCT GTT GTG AAG CTA ATG -3' |
| *GSTA1* Reverse | 5'- GGA TGG TAA CTC TTC TCC TGT G -3' |
| *GSTA4* Forward | 5'- GGA TCT GCT GGA ACT GCT TAT -3' |
| *GSTA4* Reverse | 5'- CTA GGA ACA CAC TGT CAC TCA C -3' |
| *GSTK1* Forward | 5'- CAT CCA GAG ATG CTG GAG AAA G -3' |

| | |
|---|---|
| *GSTK1* Reverse | 5’- CAT CCG GTC AGA GCC AAA TAA -3’ |
| *GSTM2* Forward | 5’- TAG TGC CTG GAA TGT AGT AGG A -3’ |
| *GSTM2* Reverse | 5’- CAG AGG CAG AGG AGA ACA AAG -3’ |
| *GSTM3* Forward | 5’- AGT TGA GGC CAG GAG TTT AAG -3’ |
| *GSTM3* Reverse | 5’- TCC CTC CAG ACT CTT CTC TAT G -3’ |
| *GSTO1* Forward | 5’- AGC TTG ACT CTT CCC TTT GG -3’ |
| *GSTO1* Reverse | 5’- GGT ATG CTT CAT CCA GGT ACT C -3’ |
| *GSTP1* Forward | 5’- CCC TAC ACC GTG GTC TAT TTC -3’ |
| *GSTP1* Reverse | 5’- GTG CCT TCA CAT AGT CAT CCT -3’ |
| *GSTT2* Forward | 5’- TCT CGG CTA TGA ACT GTT TGA G -3’ |
| *GSTT2* Reverse | 5’- TTC ACA TGA AGC TGG AGA GAA G -3’ |
| *GSTZ1* Forward | 5’- GCT AGG TAA GGA AAG GGA GTT G -3’ |
| *GSTZ1* Reverse | 5’- CCA GCG ATG AGG TCA GAA AT -3’ |

*Assays for* GSH *Protein and* GST *Enzyme Activity*

Evaluation of GSH levels were performed using the DetectX Glutathione Fluorescent Detection kit (Arbor Assays) using cell lysates. Cells were counted, aliquoted and pelleted. After removal of the supernatant, cells were stored at -80°C dry. Lysis was completed with resuspension in cold 5% aqueous 5-sulfo-salicylic acid dihydrate(Sigma-Aldrich) at a concentration of 1 x $10^6$ cells/mL. Lysates were centrifuged at 14,000 rpm for 10 minutes at 4°C. The supernatant was diluted 1:4 with supplied assay buffer. The

assay was performed in a flat black Corning Costar half area 96 -well plate with 50 µL samples and 25 µL Thiostar reagent. A fluorescent product is formed by covalent bonding to the free thiol group on GSH. After 15-minute incubation, free GSH levels were determined by fluorescent emission readings at 505 nm with excitation at 400 nm on an Infinite F200 plate reader (Tecan). Total GSH readings were obtained after an additional 15-minute incubation with the NADPH/Glutathione Reductase reaction mixture.

GST enzyme activity levels were measured using the DetectX Glutathione S-Transferase Fluorescent Activity kit (Arbor Assays) using cell lysates with 1 x $10^6$ cells/mL. Cells were prepared and stored at -80°C dry as noted for the GSH assay. Frozen, lysed cells were resuspended at 1 x $10^6$ cells per mL in provided assay buffer and vortexed vigorously. Lysates were centrifuged at 14,000 rpm for 10 minutes at 4°C. A flat black Corning Costar half area 96 -well plate was prepared with 50 µL samples and 25 µL of provided detection reagent. Equal quantities of GSH were added to each well to yield a fluorescent product read at 465 nm with excitation at 400 nm on an Infinite F200 plate reader (Tecan).

*Statistical Analysis*

Statistical analysis includes Excel for unpaired student T test and standard error. Minitab 18 is used for one-way ANOVA, Tukey and Fisher pairwise comparison, as well as Tukey and Fisher Simultaneous Tests for Differences of Means. Jamovi is used for repeated measures ANOVA analysis. MyAssays.com is used for analysis of raw data

from the DetectX Glutathione Fluorescent Detection kit and the DetectX Glutathione S-Transferase Fluorescent Activity kit.

# RESULTS

## Characteristics of IPF and Normal Fibroblasts

*Determination of GST isoforms in IPF and Normal fibroblast*

The *GST* isoform profile for IPF and Normal fibroblast was determined by qPCR. After screening, only GST isoforms with threshold cycle (Ct) levels below 30 were considered for further study [60]. The *GSTA4, GSTK1, GSTM3, GSTP1* and *GSTT2* isoforms all passed this threshold and were considered for further study.

*GST Profile: Gene Expression in Control Fibroblasts*

The initial *GST* expression profile (n = 3) provides a baseline comparison calculated as an expression score of $1x10^5/2^{\Delta CT}$ (Figure 8). While there is no significant difference in *GST* isoform expression between IPF fibroblast and normal fibroblast prior to treatment, each isoform demonstrates a specific expression profile. *GSTP1* is expressed at the highest levels in both normal fibroblasts (267.3 ±66.5) and IPF fibroblasts (529.2 ±182.1). *GSTP1* expression is more than four times that of any other isoform. The second highest expression score is *GSTK1* in both normal fibroblast (64.5 ±13.3) and IPF fibroblast (95.3 ±20.8). *GSTT2* average expression is 19.7 ±8.2 in normal fibroblast and 14.7 ±2.5 in IPF fibroblast. *GSTA4* expression scores in normal fibroblast (2.2 ±0.4) and IPF fibroblast (5.0 ±1.8) are higher than the *GSTM3* expression scores in normal fibroblast (1.4 ±0.2) and IPF fibroblast (2.2 ±0.4). (Appendix B)

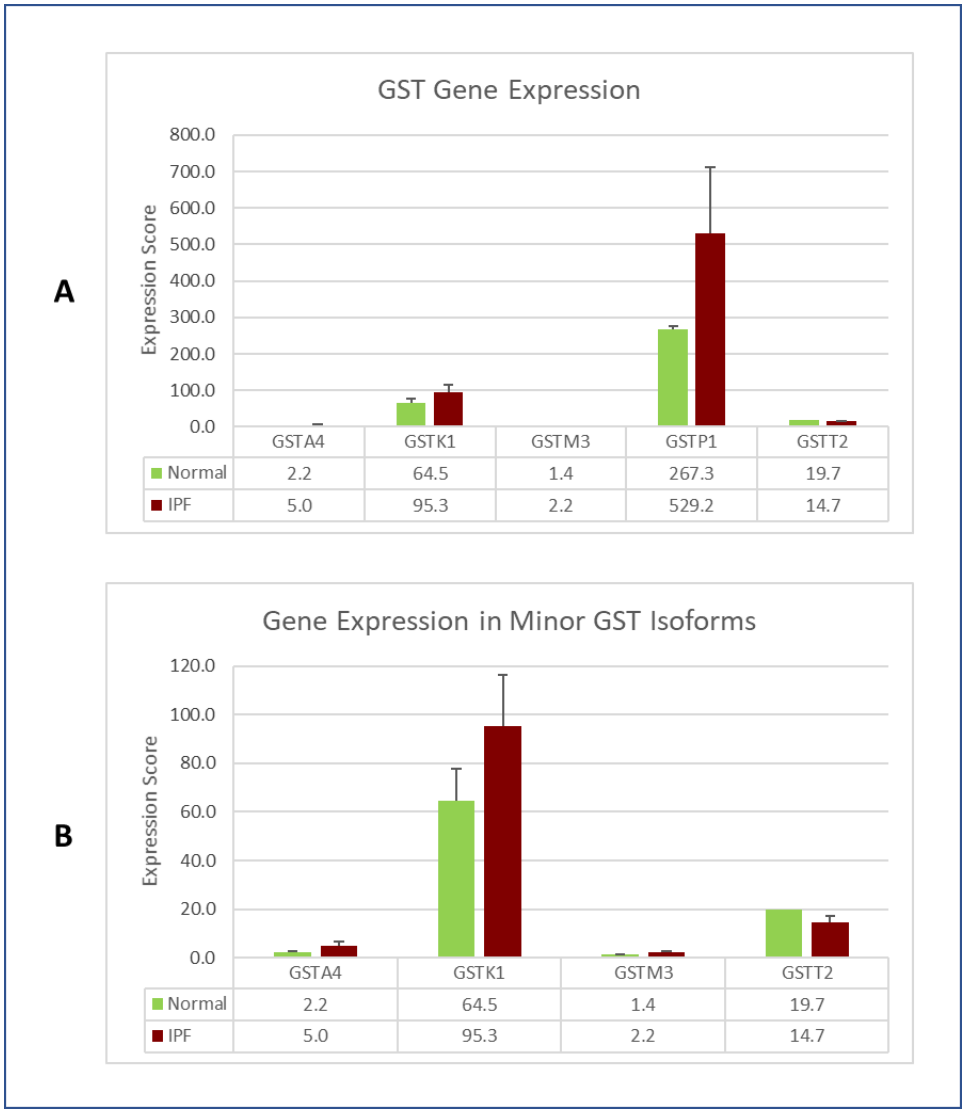


**Figure 8 *GST* Gene Expression Profile**

**The relative expression of *GST* isoforms is presented as expression scores ($1x10^5/2^{\Delta CT}$) creating a baseline expression profile (n = 4). No significant difference is found between normal fibroblast and IPF fibroblast, but clear differences are seen between GST isoforms. *GSTP1* has the highest expression scores in both normal fibroblasts (267.3 ±66.5) and IPF fibroblasts (529.2 ±182.1). The second highest expression score is *GSTK1* in both normal fibroblast (64.5 ±13.3) and IPF fibroblast (95.3 ±20.8). *GSTT2* is followed by *GSTA4* and *GSTM3*.**

### *Activity Profile:* GST *Activity and* GSH *Levels*

#### *Validation of* GST *Activity Assay and* GSH *Assay*

To determine the correct concentration of cell lysate required to assay the levels of GSH and total GST enzyme activity serial dilutions of fibroblast cells were lysed and used for preliminary assays (Figure 9). A concentration of $1 \times 10^6$ fibroblasts per mL is in the linear range of the standards and was used for both assays.

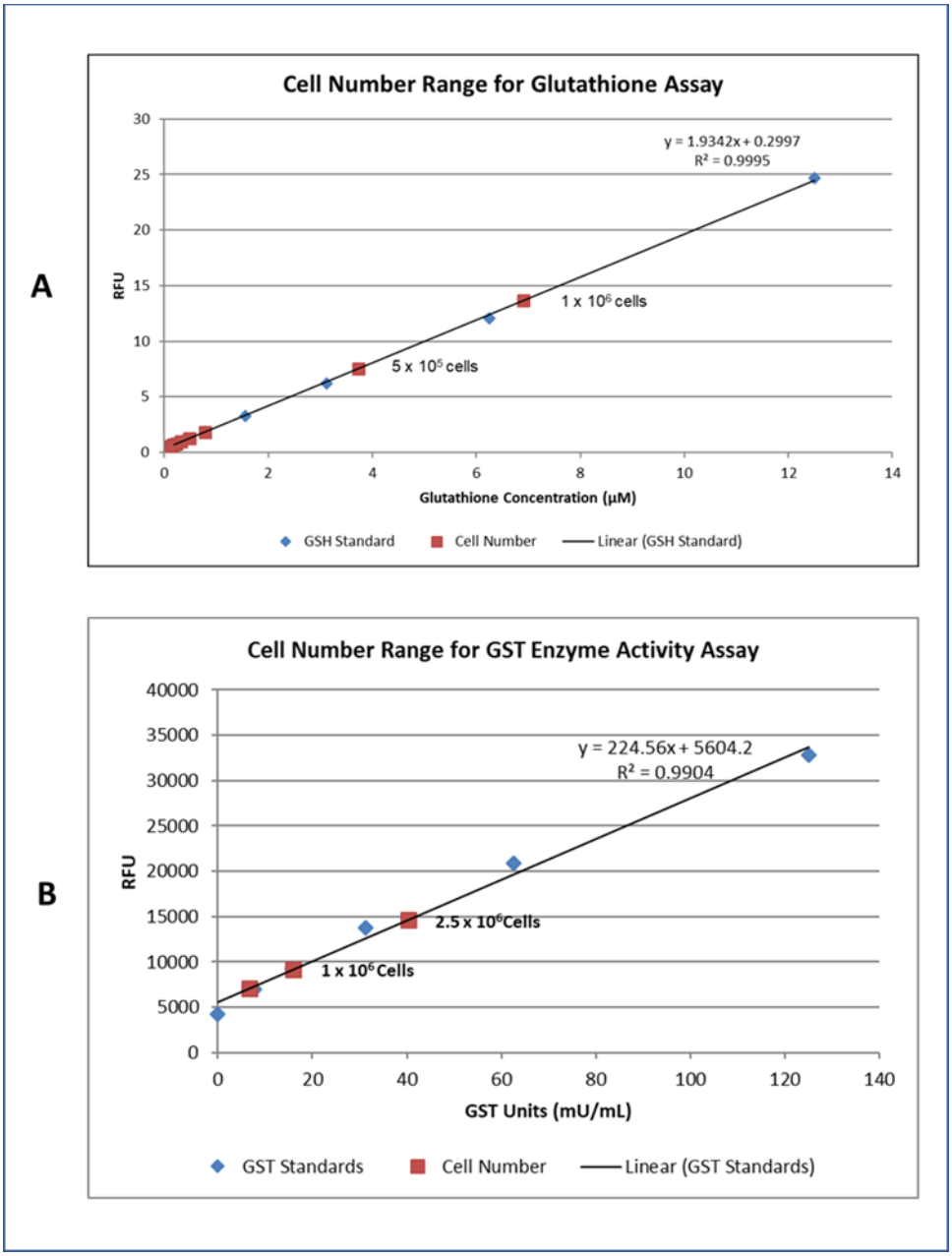


**Figure 9 Cell Number for Assays**
**A concentration of 1 x $10^6$ fibroblast cells per mL is in the linear range for both the assay for (A) GSH concentration and (B) the assay measuring total GST enzyme activity.**

GST *Enzyme Activity in Control Fibroblasts*

Analysis of the total GST enzyme activity is accomplished by measuring GSH-GST conjugation to form a fluorescent reporter molecule and comparing to GST enzyme standards. Assessment of control cells reveals that IPF fibroblasts display significantly higher total GST enzyme activity at 50 ±5.2 mU/mL (Figure 10) compared to normal fibroblasts at 20 ±4.1 mU/mL ($p < 0.000$) ($n = 3$). (Statistical Analysis Appendix H)

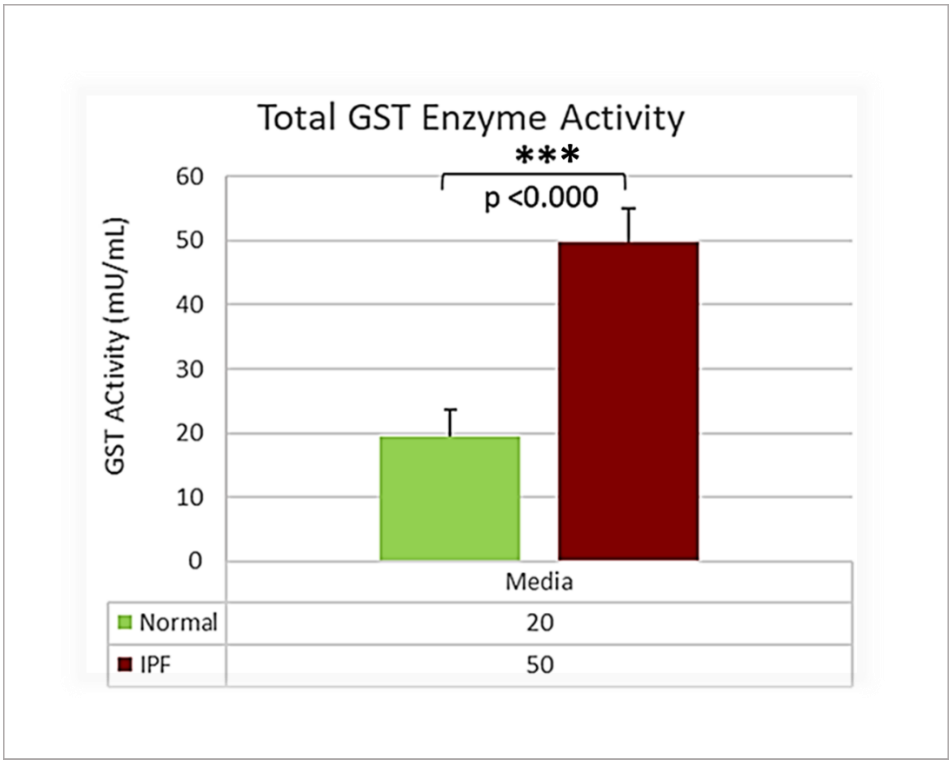


**Figure 10 GST Enzyme Activity Normal vs. IPF**
**In control conditions, IPF fibroblasts display 2.5 times the total GST enzyme activity of normal fibroblasts, 50 ±5.2 mU/mL compared to 20 ±4.1 mU/mL ($p < 0.000$) ($n = 3$).**

### *Assessment of* GSH *levels in Control Fibroblasts*

Analysis of the GSH concentration reveals that normal fibroblasts average 14.41 ±0.9 µM total GSH and 14.33 ±0.8 µM of free, or reduced GSH (Figure 11). IPF fibroblasts average 13.87 ±2.4 µM total GSH and 13.43 ±2.3 µM free GSH. The difference between IPF and normal fibroblast levels is not significant (n = 3). (Statistical Analysis Appendix G)

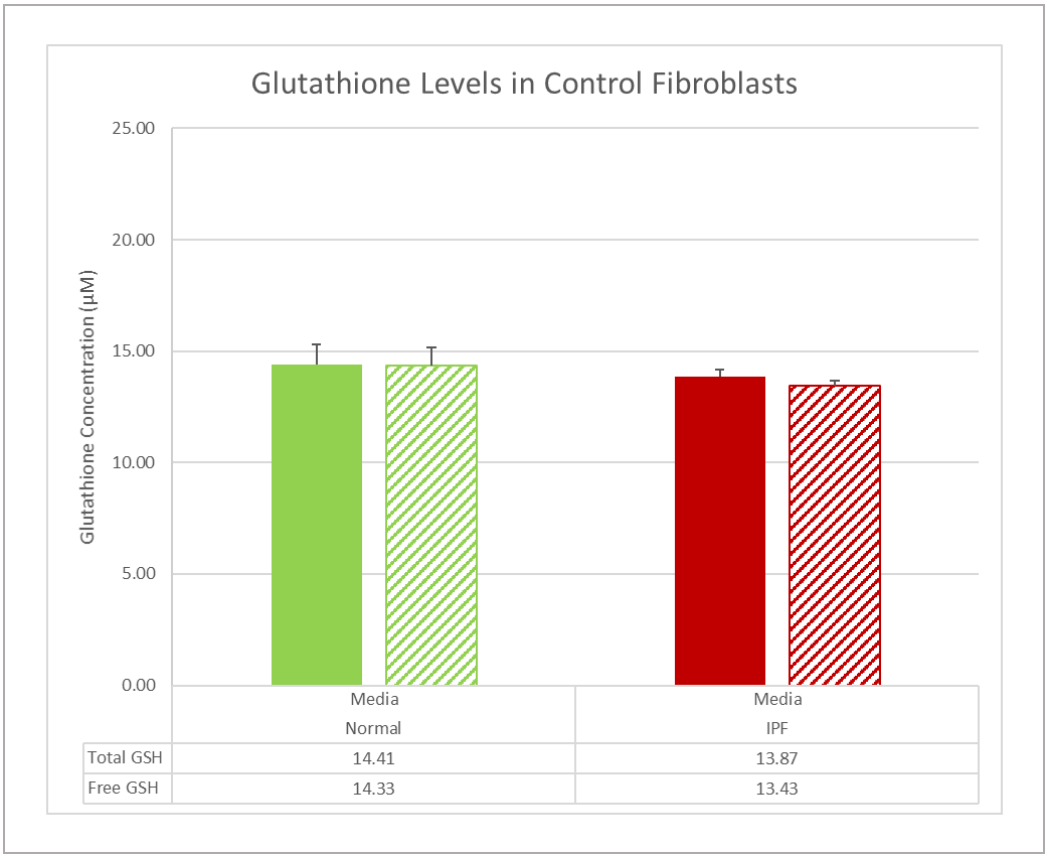


**Figure 11 GSH levels in Control Fibroblasts**
**Normal fibroblasts possess 14.41 ±0.9 µM total GSH and 14.33 ±0.8 µM free GSH. IPF fibroblasts have 13.87 ±2.4 µM total GSH and 13.43 ±2.3 µM free GSH. The difference between IPF and normal fibroblast levels is not significant (n = 3).**

*Activation Assessment of Control Fibroblasts*

In addition to high levels of GST enzyme activity, IPF fibroblasts express significantly higher levels of general markers of activation associated with differentiated myofibroblasts (Figure 12). The IPF fibroblast expression score for *ACTA2* (132.0 ±44.2) is five times the expression score for normal fibroblasts (26.5 ±9.5) (n = 4). The IPF fibroblast expression score for *COL1A1* (49.8 ±22.8) more than eight times the score for normal fibroblasts (7.7 ±1.4). (Appendix B)

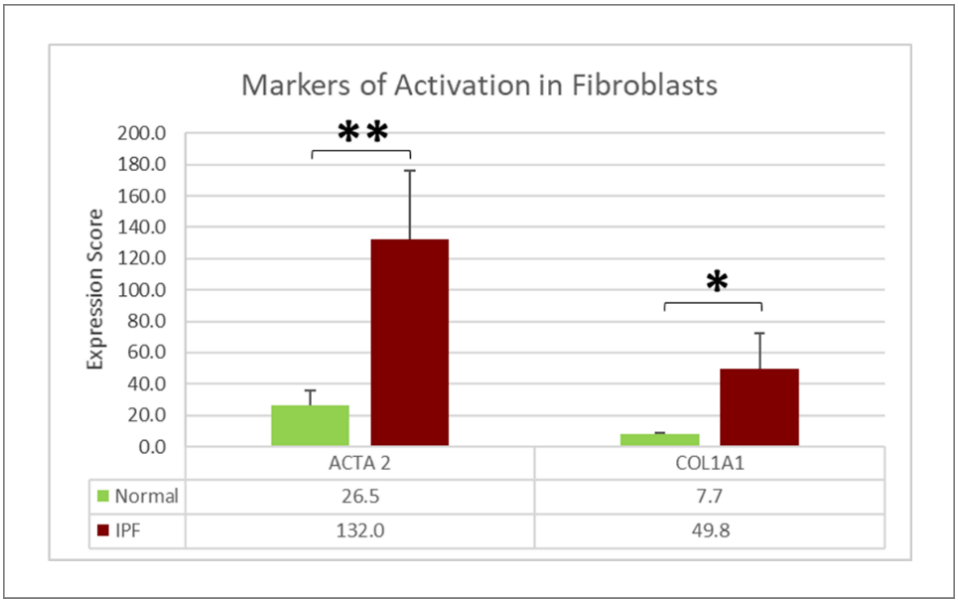


**Figure 12 Activation Markers IPF vs. Normal**
**The IPF fibroblast expression score for *ACTA2* (132.0 ±44.2) is five times the expression score for normal fibroblasts (26.5 ±9.5). The IPF fibroblast expression score for *COL1A1* (49.8 ±22.8) more than eight times the score for normal fibroblasts (7.7 ±1.4). The differences in both markers for activation are significant in control conditions (*ACTA2* p = 0.008; *COL1A1* p = 0.012) (n = 4).**

## GST and Oxidative Stress

### *Determination of $H_2O_2$ Concentrations*

Preliminary $H_2O_2$ toxicity tests were carried out to identify two $H_2O_2$ concentrations. The low $H_2O_2$ concentration must be capable of simulating the stressful, oxidative environment found in IPF lungs but not so toxic as to disallow sufficient cells for analysis [22]. The high $H_2O_2$ concentration must characterize the differential survival between cell types [20]. Cell viability is significantly lower ($p=0.002$) at 1mM concentration (Figure 13) providing a concentration appropriate for cell survival assessment. The 200 μM concentration was selected to deliver the low level oxidative stress conditions desired. (Statistical Analysis Appendix A)

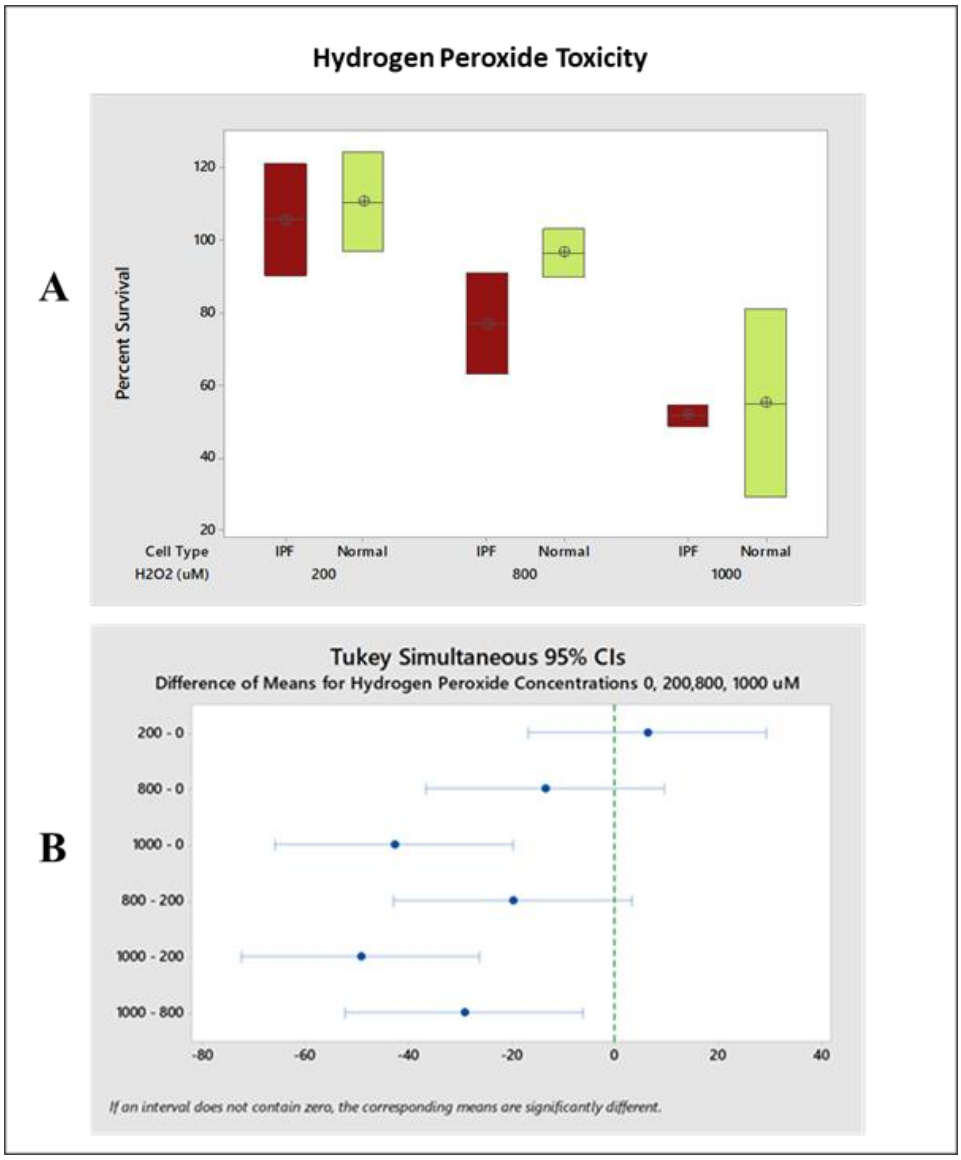


**Figure 13 Hydrogen Peroxide Toxicity**
**A) Initial range finding for $H_2O_2$ survival shows 200 µM $H_2O_2$ with IPF fibroblasts = 105.7 ±15.4% and Normal fibroblasts = 110.6 ±13.9%. The 800 µM $H_2O_2$ survival is IPF fibroblasts = 77 ±13.9% and Normal fibroblasts = 96.6 ±6.7% and 1000 µM $H_2O_2$ survival is IPF fibroblasts = 51.8 ±3.0% and Normal fibroblasts = 55.1 ±25.9%. B) Tukeys difference of the means indicates 200 µM $H_2O_2$ shows no significant difference from media control (p = 0.4). The 1 mM $H_2O_2$ concentration is appropriate for the survival assay (p = 0.002) indicating mean survival for 1 mM $H_2O_2$ is statistically different from media control and provides sufficient cell death to identify meaningful differences.**

*Differential Survival of IPF Fibroblasts after $H_2O_2$ Challenge*

The evaluation of cell survival when challenged with 1 mM $H_2O_2$ indicates enhanced and significant survival (p = 0.031) in the IPF fibroblasts compared to normal fibroblasts (n=10). IPF fibroblasts survival in the presence of 1 mM $H_2O_2$ is 74% ±3.25; and 63% ±3.01 for normal fibroblasts (Figure 14). Survival data demonstrates IPF fibroblast resistance to cell death induced by $H_2O_2$ challenge as compared to normal fibroblasts. (Statistical Analysis Appendix C)

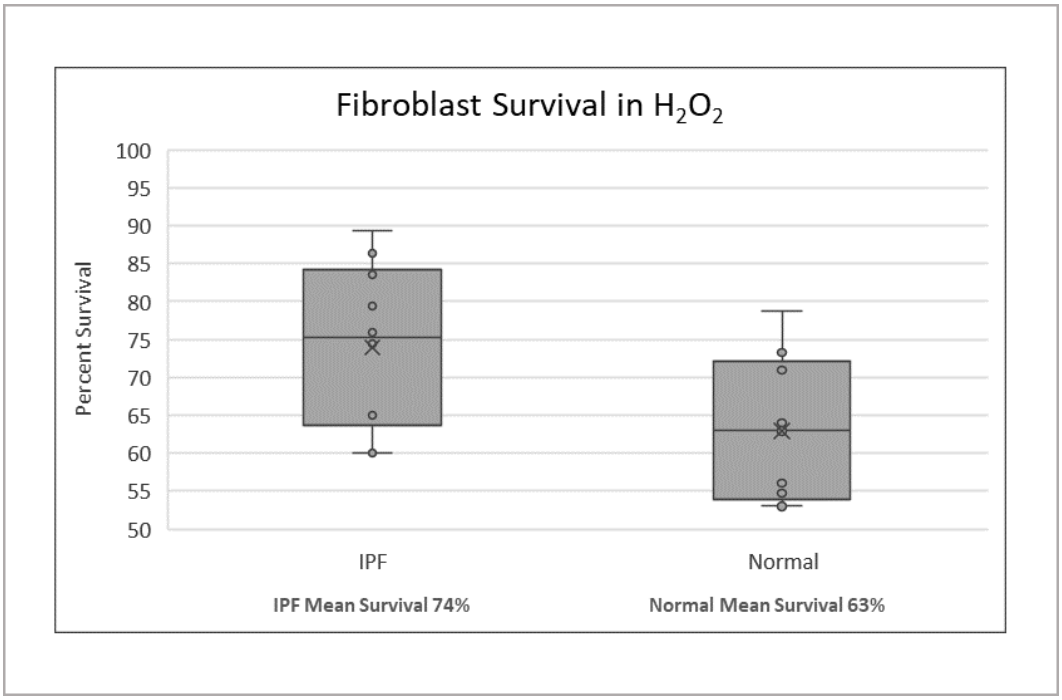


**Figure 14 Summary of 1 mM $H_2O_2$ Survival**
**Baseline survival in fibroblast shows IPF fibroblast (n = 10) mean survival at 74% ±3.25 and 63% ±3.01 for normal fibroblasts (p = 0.03).**

*Cell Survival and GST Expression*

We further examine the resistance to cell death under $H_2O_2$ challenge. If GSTs support enhanced survival in IPF fibroblasts, then GST expression levels should increase in response to $H_2O_2$ stress. qPCR analysis (n=4) shows that all GST isoforms studied increase in response to moderate 200 μM $H_2O_2$ conditions in both IPF and normal fibroblasts (Figure 15). A point of distinction is the significant difference in expression ($p = 0.03$) in *GSTA4* by IPF fibroblasts (1.88 fold) compared to normal fibroblasts (1.33 fold). However, only the IPF fibroblasts increase *GSTA4* significantly ($p = 0.005$) in $H_2O_2$ compared to control. *GSTM3* increases expression in $H_2O_2$ significantly in both normal fibroblasts (1.5 fold; $p = 0.03$) and IPF fibroblasts (1.38 fold; $p = 0.01$). Only normal fibroblasts significantly increase *GSTT2* expression (1.78 fold; $p = 0.05$) in $H_2O_2$. The increases in GSTP1 found in IPF fibroblast (1.31 fold) and normal fibroblast (1.17 fold) are not significantly different. However, in the GST expression profile of control cells (Figure 8), the initial *GSTP1* expression score was four-fold greater than any other GST isoform. This implies that a fold increase in *GSTP1* expression corresponds to larger quantities of mRNA than do fold increases in the other GST isoforms, supporting the critical role of GSTP1. (Appendix F)

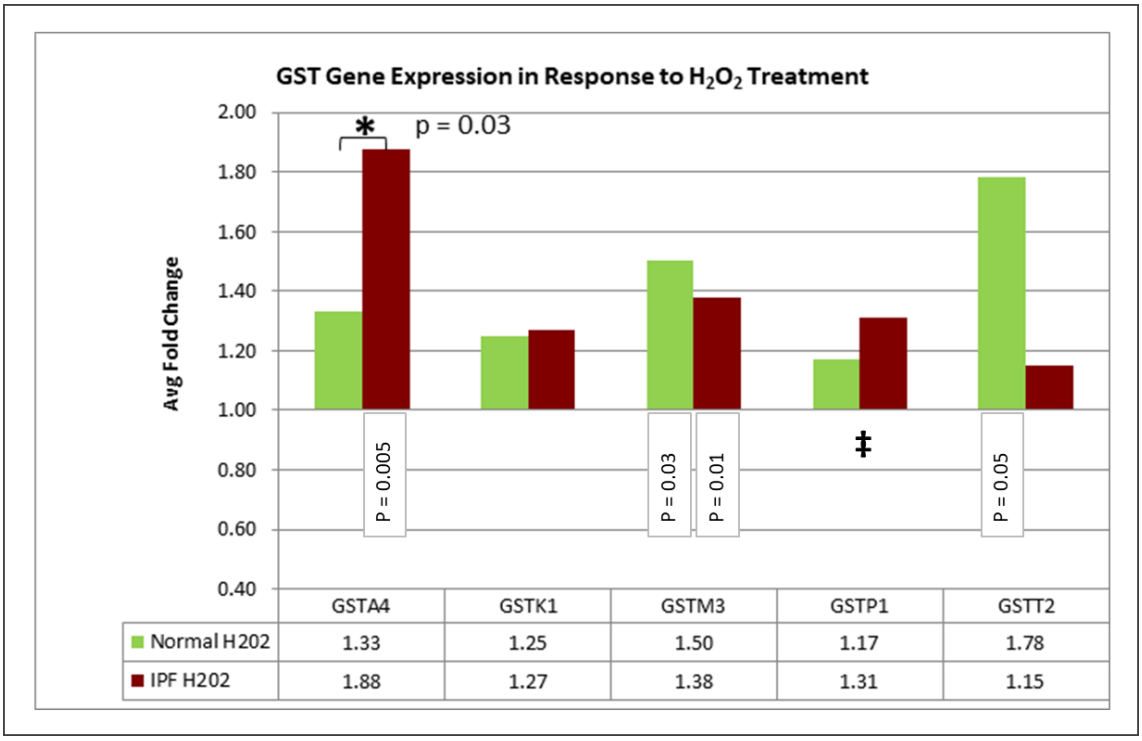


**Figure 15 *GST* Gene Expression Response to $H_2O_2$**
**Exposure to 200 µM $H_2O_2$ increases expression of all GST isoforms in both IPF and normal fibroblast (n=4). IPF fibroblasts increase in *GSTA4* significantly (1.88 fold; p = 0.005) in $H_2O_2$ compared to control. The increase in *GSTA4* creates a significant difference (p = 0.03) between IPF fibroblasts and normal fibroblasts. *GSTM3* increases significantly in both normal fibroblasts (1.5 fold; p = 0.03) and IPF fibroblasts (1.38 fold; p = 0.01). Only normal fibroblasts significantly increase *GSTT2* expression (1.78 fold; p = 0.05).**
**‡ The initial *GSTP1* expression score, four times all other GSTs, indicates fold increases in *GSTP1* expression correspond to vastly larger quantities of mRNA.**

*Effect of $H_2O_2$ on* GST *Enzyme Activity*

GST activity in IPF cells is significantly greater than in normal fibroblasts and is a combination of total activity for all the GST isoforms. The GST enzyme activity after 200 µM $H_2O_2$ stress clearly demonstrates superior total GST enzyme activity in IPF fibroblasts (Figure 16). IPF fibroblast activity increased from 50 ±5.2 mU/mL to 59 ±14.7 mU/mL GST enzyme standard activity, while normal fibroblast total activity

decreases significantly from 20 ±4.1 mU/mL to 15 ±3.5 mU/mL enzyme (p = 0.0000009) (n = 3). The gene expression increases of *GSTP1*, *GSTK1* and *GSTA4* in IPF fibroblast correlate with increased GST enzymatic activity and contributes to IPF fibroblast resistance to cell death. (Statistical Analysis Appendix H)

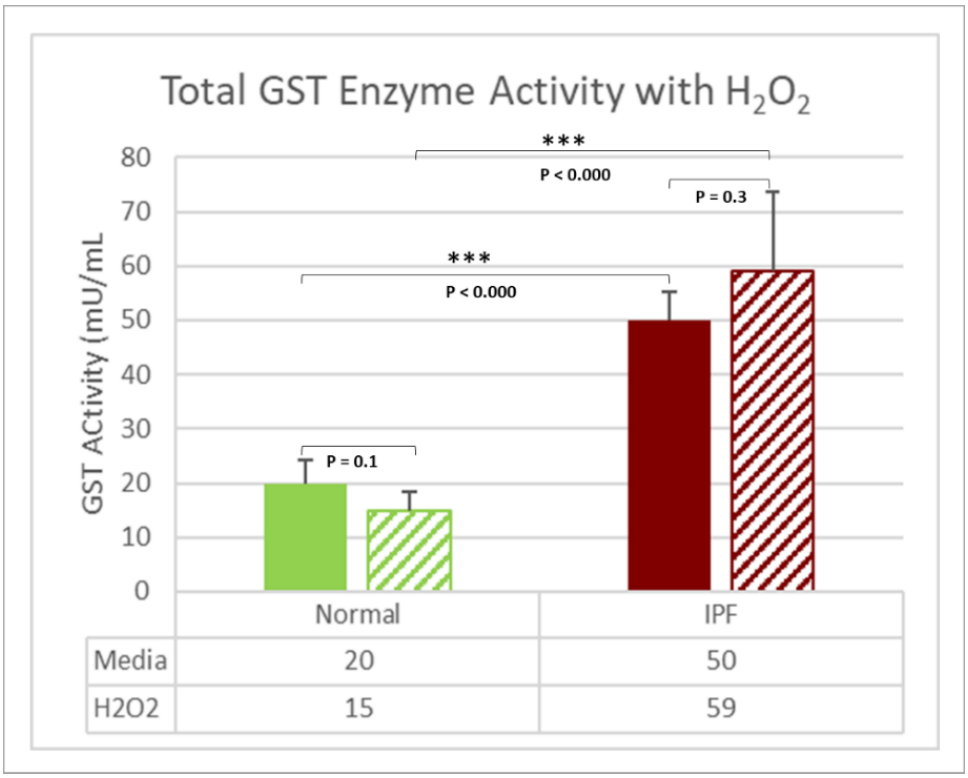


**Figure 16 Differential GST Enzyme Activity with $H_2O_2$**
**Treatment with 200 µM hydrogen peroxide produces GST enzyme activity in normal fibroblasts of 15 ±3.5 mU/mL. However, IPF fibroblasts possess GST enzyme activity of 59 ±14.7 mU/mL. Hydrogen peroxide stress increases the significant difference in GST enzyme activity (p= 0.0000009) (n=3).**

## Inhibition of GSTP

We propose that GSTP1, as the major GST isoform present in lung fibroblasts, plays a critical role in the ability of IPF activated myofibroblasts to persist in the oxidative environment of the IPF lung. Therefore, inhibition of GSTP1 should modify IPF fibroblasts to behave like normal fibroblasts. To determine the contribution of GSTP1, cells are pretreated with the GSTP1 inhibitor TLK199 at sub-lethal concentrations prior to 200 μM $H_2O_2$ exposure for qPCR and 1mM $H_2O_2$ for survival assays.

### *Identification of Appropriate Inhibitor Concentration*

Initial toxicity testing determined that 50 μM TLK199 was not lethal and exhibits differential effects in the cell lines utilized in this study (Figure 17). (Statistical Analysis Appendix D)

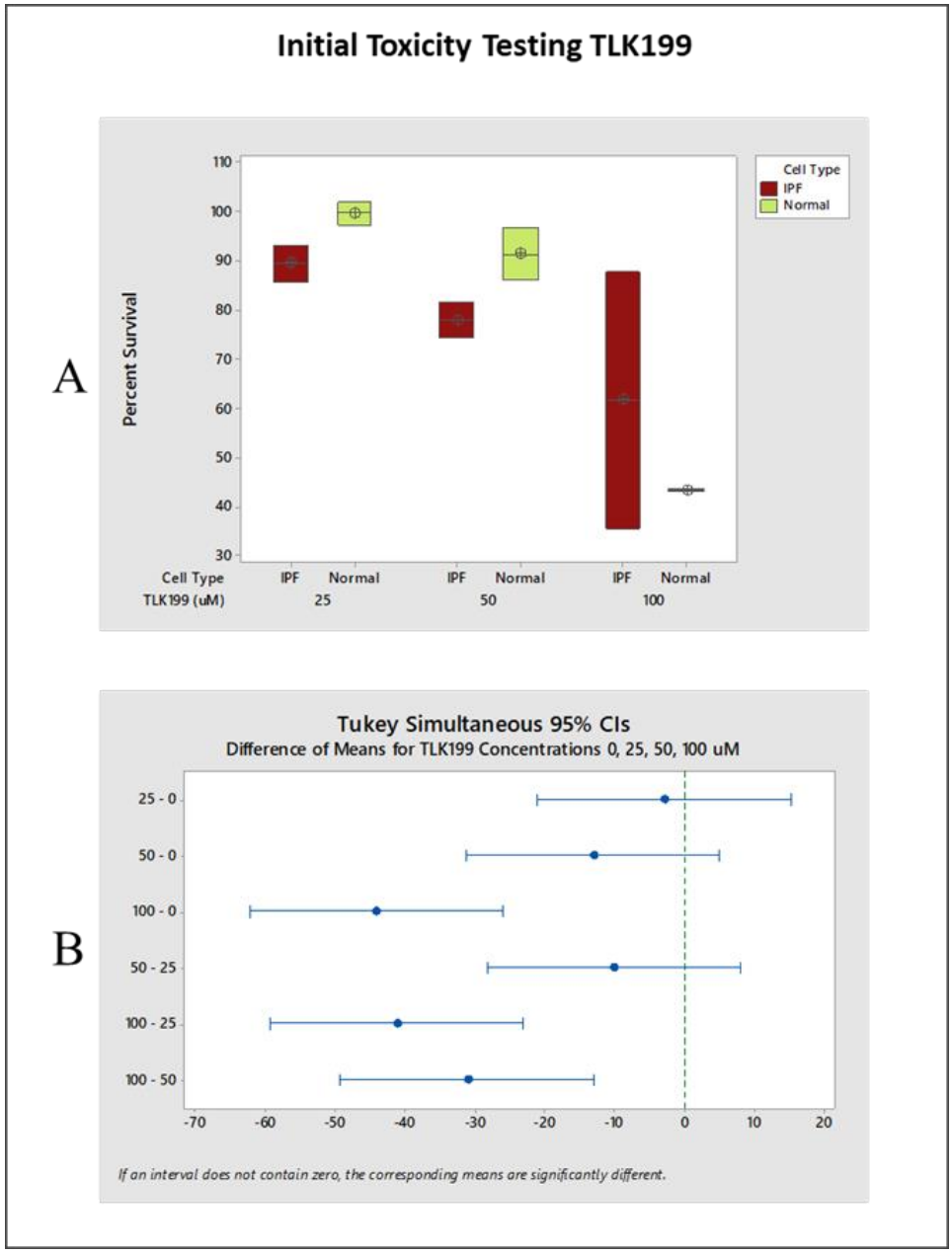


**Figure 17 Initial TLK 199 Toxicity Screening**
**A) Percent survival in IPF fibroblasts and normal fibroblasts for increasing concentrations of TLK199 indicate minor effects up to the 100 µM concentration. B) One-way ANOVA with both Tukey and Fisher pairwise comparison (Appendix D) show mean survival for 25 µM TLK199 ($p = 0.9$) and 50 µM TLK199 ($p = 0.2$) are not significantly different from media control. However, 100 µM TLK199 leads to a substantial drop in survival rate ($p < 0.001$). The 50 µM TLK199 concentration meets the goal for the inhibitor to exhibit differential effects in surviving cells.**

*Effect of* GSTP1 *Inhibitor on Total* GST *Enzyme Activity*

The modification of IPF fibroblast performance to near normal fibroblast values is observed in the assay for total GST enzyme activity (Figure 18). After sequential TLK199/$H_2O_2$ treatment, IPF fibroblasts show a decrease in total GST enzyme activity from 59 ±14.7 mU/mL to 39 ±3.7 mU/mL ($p = 0.049$). Whereas, normal fibroblasts demonstrate an increase in total GST enzyme activity from 15 ±3.5 mU/mL to 27 ±9.7 mU/mL ($p = 0.035$). GSTP1 inhibition removes the significant difference in total GST activity between IPF and normal fibroblast ($n = 3$) ($p = 0.05$; Tukey Simultaneous Tests for Differences of Means $p = 0.485$; Statistical Analysis Appendix H).

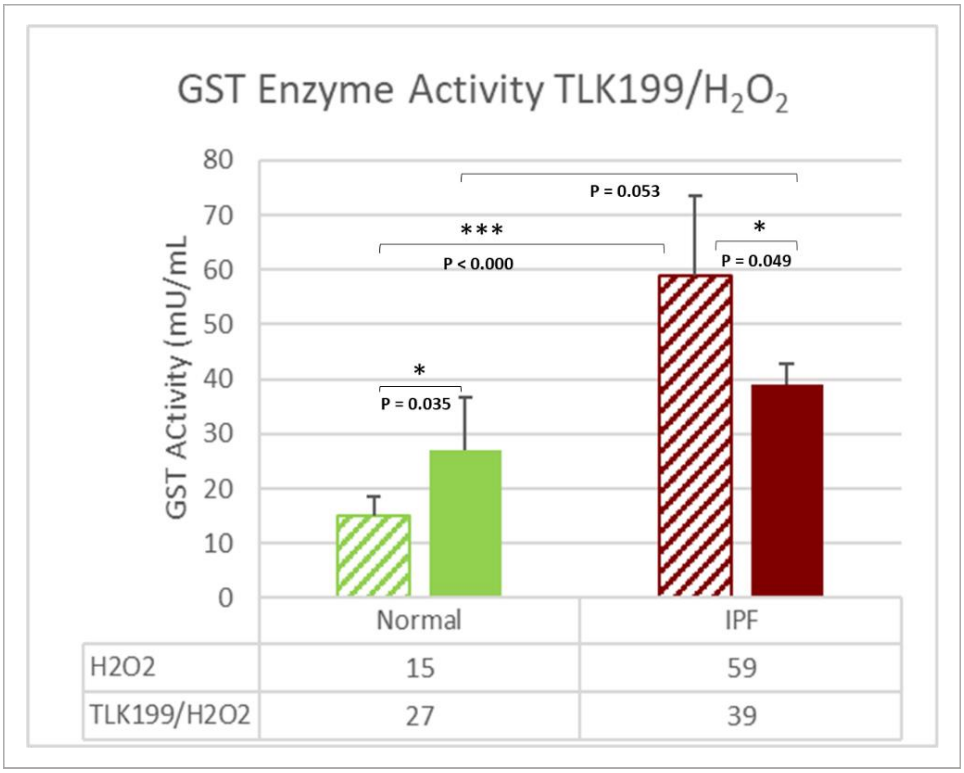


**Figure 18 GST Activity after $H_2O_2$/TLK199**
**IPF fibroblasts after TLK199/$H_2O_2$ treatment reduce total GST enzyme activity from 59 ±14.7 to 39 ±3.7 mU/mL (p = 0.049). Normal fibroblasts demonstrate an increase from 15 ±3.5 to 27 ±9.7 mU/mL of total GST enzyme activity (p = 0.035). The difference between IPF and normal fibroblasts diminishes (p = 0.053) (n = 3).**

*Effect of* GSTP1 *Inhibitor TLK199 on Expression of GSTs*

An examination of *GST* gene expression changes after inhibitor aids our understanding of why GSTP1 seems essential for normal fibroblast survival yet appears only moderately important to IPF fibroblast survival. After TLK199 pretreatment (Figure 19), normal fibroblasts decrease expression of *GSTA4* (0.82 ±0.2 fold) while IPF fibroblasts maintain the increase (1.97 ±0.6 fold) provoked by $H_2O_2$ alone (Figure 15) resulting in a difference of high significance ($p = 0.001$). *GSTK1* follows this same pattern, a decrease in normal fibroblast expression (0.9 ±0.1 fold) but an increase in IPF fibroblast expression (1.59 ±0.4 fold; $p = 0.018$). *GSTP1* expression decreases only in normal fibroblasts (0.94 ±0.2 fold) with TLK199/$H_2O_2$ treatment. *GSTP1* expression increases (1.45 ±0.5 fold) in IPF fibroblasts ($p = 0.03$). Keeping in mind the initial GST profile expression score for *GSTP1* (Figure 8) was four times the next *GST* isoform (*GSTK1*), we see a differential response to GSTP1 enzyme inhibition in IPF cells and a potential reason why GSTP1 appears only moderately important to the survival of IPF fibroblasts. When the major GST isoform is inhibited, IPF fibroblasts respond by increasing expression of *GSTA4*, *GSTK1* and *GSTP1* whereas normal fibroblasts do not. (Appendix F)

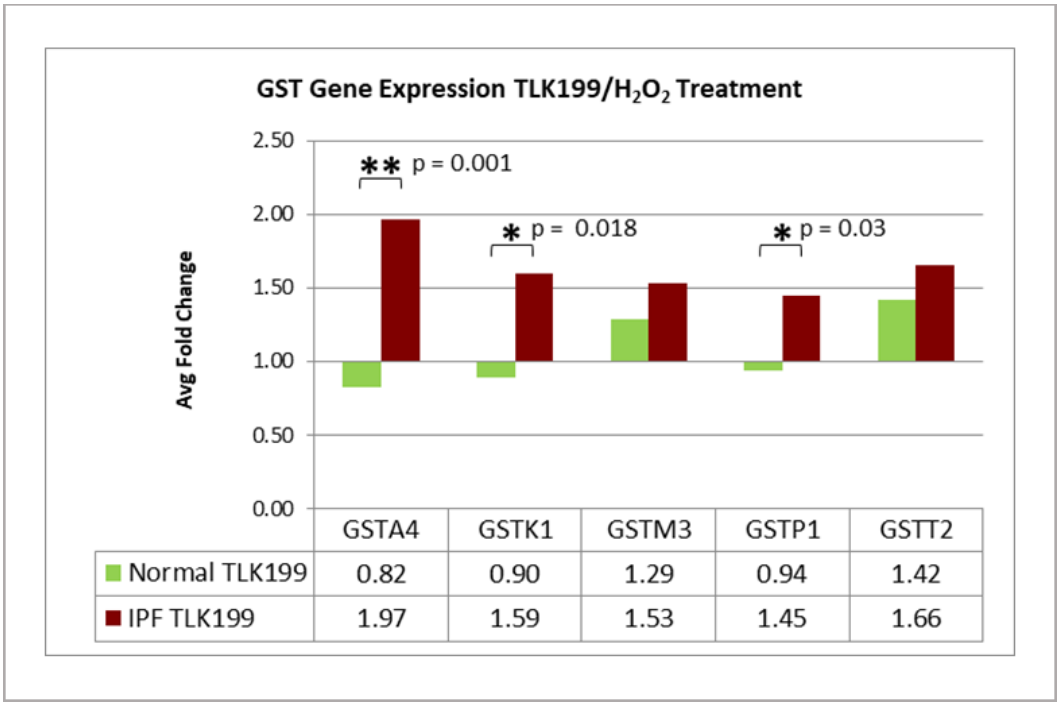


**Figure 19 *GST* Gene Expression Response to TLK199/$H_2O_2$**
**TLK199 pretreatment prior to $H_2O_2$ decreases expression of *GSTA4* in normal fibroblasts (0.82 ±0.2 fold) while increasing *GSTA4* expression in IPF fibroblasts (1.97 ±0.6 fold) with a significant difference (p = 0.001). *GSTK1* expression decreases (0.9 ±0.1 fold) in normal fibroblast but increases in IPF fibroblasts (1.59 ±0.4 fold) producing a significant difference (p = 0.018). *GSTP1* expression also decreases in normal fibroblasts (0.94 ±0.2 fold) but increases (1.45 ±0.5 fold) in IPF fibroblasts (p = 0.03) (n = 4).**

*Effect of TLK199 Pre-treatment on Survival*

Exposure of IPF fibroblasts to the GSTP1 inhibitor resulted in a decrease in total GST activity (Figure 18) essentially normalizing the GST total activity between normal and IPF fibroblasts. To test out hypothesis that GSTP1 plays a critical role in the ability of IPF fibroblasts to function and survive in the hostile environment of the IPF lung and survival levels determined.

Cells were pretreated with a sub-lethal concentration GSTP1 inhibitor TLK199 prior to 1 mM $H_2O_2$ exposure for sixteen hours (n = 4). This reduced mean IPF fibroblast cell survival (Figure 20) from 73.9% ±3.2 to 40.6% ± 7.4 ($p = 0.0004$). Normal fibroblast mean survival dropped from 62.9% ±3.0 survival to 14.6% ± 9.5 ($p = 0.00007$). One-way ANOVA analysis of survival by cell type with TLK199 inhibitor indicates no statistical difference ($p = 0.1$) between IPF fibroblast mean survival and normal fibroblast mean survival (Statistical Analysis Appendix E). GSTP Inhibition with TLK199 mitigates the IPF fibroblast survival advantage. GSTP1 appears almost essential for normal fibroblast survival with a 48% drop in survival after TLK199 inhibitor. In IPF cells, the 33% decrease in mean survival indicates moderate importance for GSTP1 in IPF fibroblast mean survival.

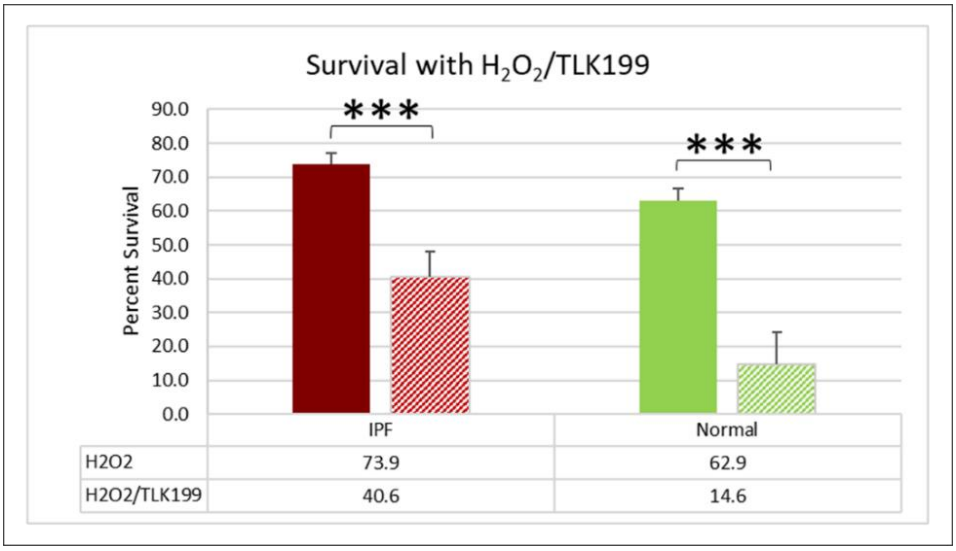


**Figure 20 TLK199 Reduces Survival**
**Inhibition of GSTP1 using TLK199 prior to 1 mM $H_2O_2$ exposure reduces IPF fibroblast cell survival from 73.9% ±3.2 to 40.6% ± 7.4 (p = 0.0004). Normal fibroblast survival dropped from 62.9% ±3.0 survival to 14.6% ± 9.5 (p = 0.00007). One-way ANOVA analysis indicates no statistical difference (p =0.1) between IPF fibroblast mean survival and normal fibroblast mean survival after TLK199/$H_2O_2$ (n = 4) (Statistical Analysis Appendix E).**

*No Change in Fibroblast Activation with Treatment*

IPF fibroblasts express significantly higher levels of mRNA markers associated with the myofibroblast phenotype compared to normal fibroblasts (Figure 12). While TLK199 appears to normalize IPF fibroblasts in areas related to survival, the IPF fibroblasts are not necessarily inactivated by GSTP1 inhibition. True dedifferentiation from activated myofibroblast to inactive fibroblast must be assessed via markers of activation. We see no change in activation markers with $H_2O_2$ or TLK199/$H_2O_2$ treatment (Figure 21) (n = 4). $H_2O_2$ does not increase activation of either normal fibroblasts or IPF fibroblasts. The baseline expression scores for markers of activation (Figure 12) indicated IPF fibroblast *ACTA2* expression is five times that of normal fibroblasts. The baseline expression score for *COL1A1* in IPF fibroblasts is eight times the normal fibroblast expression score. While there is some variation in mRNA levels for *ACTA2* and *COL1A1*, no significant difference is found for $H_2O_2$ or TLK199/$H_2O_2$ treatment (Figure 21). IPF fibroblasts maintain high activation status while normal fibroblasts retain lower activation.

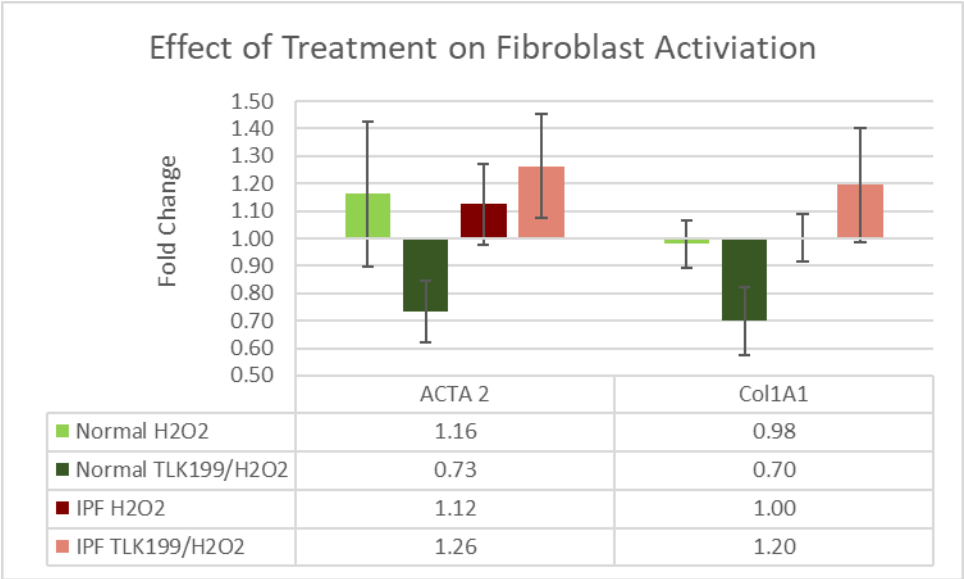


**Figure 21 Effect of $H_2O_2$ and TLK199/$H_2O_2$ on Fibroblast Activation**
**Treatment with $H_2O_2$ or TLK199/$H_2O_2$ results in minor variation of *ACTA2* and *COL1A1* mRNA levels (n = 4). No significant change in expression of activation markers is seen.**

*TLK199 does not Impact Intracellular Glutathione Concentration*

Fluctuations in the intracellular pool of free GSH and conjugated GSSG have the potential to contribute to redox regulation. Formation of GSSG from two free GSH molecules allows reduction and detoxification of ROS such as $H_2O_2$. [31]. GSH levels were assessed via fluorescent assay for all treatment groups (Figure 22). Changes in GSH levels, both free and total, were statistically insignificant (n = 3). (Statistical Analysis Appendix G)

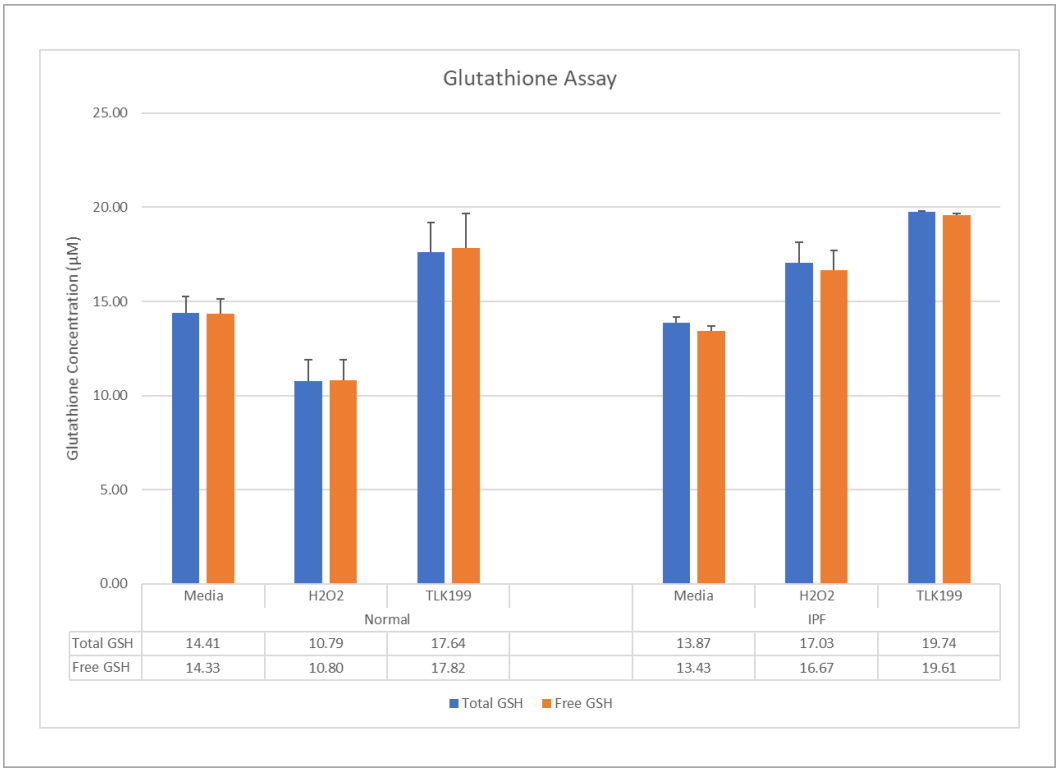


| | Normal | | | | IPF | | |
|---|---|---|---|---|---|---|---|
| | Media | H2O2 | TLK199 | | Media | H2O2 | TLK199 |
| Total GSH | 14.41 | 10.79 | 17.64 | | 13.87 | 17.03 | 19.74 |
| Free GSH | 14.33 | 10.80 | 17.82 | | 13.43 | 16.67 | 19.61 |

**Figure 22 GSH Assay**
**Analysis of both free and total GSH in fibroblasts indicate neither cell type nor treatment group exhibit significant differences (n = 3).**

*Epithelial Cells*

IPF results in cellular imbalance caused by epithelial cell death and excessive myofibroblasts that resist cell death [13]. We have demonstrated attenuation of abnormal survival in IPF fibroblasts with inhibition of GSTP1, reducing cell survival in IPF fibroblast, 65.0% to 40.6% ($p = 0.02$), and normal fibroblast, 58.4% to 14.6% ($p = 0.0007$). However, AEC are known to demonstrate $H_2O_2$ induced cell death [22]. Further increases in AEC cell death due to GSTP1 inhibition would be counterproductive. Epithelial cells are less susceptible than fibroblasts to the effects of TLK199 inhibition, 59.5% to 49.5% (Figure 23A). Epithelial cells under $H_2O_2$ stress demonstrate a decrease in *GSTP1* mRNA levels in both $H_2O_2$ and TLK199/ $H_2O_2$ (figure 23C). TLK199 pretreatment resulted in no significant difference from $H_2O_2$ alone. However, the expression score for *GSTP1* in epithelial cells (6177.6 ±1558) is more than ten times higher than that of IPF fibroblasts (529.2 ±182; $p = 0.004$) or normal fibroblasts (267.3 ±66.5; $p = 0.001$) (Figure 23B). TLK199 has no significant effect on epithelial cells due to vastly higher expression of *GSTP1*. A decrease (0.45 fold) from the epithelial cell baseline expression score is still five times greater *GSTP1* mRNA levels in epithelial cells than IPF fibroblasts. Epithelial cells after TLK199/$H_2O_2$ are still significantly different than IPF fibroblast ($p = 0.005$) and normal fibroblast ($p = 0.035$). While GSTP inhibition decreases expression in epithelial cells, mRNA levels after treatment is still sufficiently abundant that survival is not reduced in the $H_2O_2$ simulated ROS environment.


**Figure 23 Effects in Epithelial Cells**

**A) Epithelial cell survival after TLK199 inhibition declines from 59.5% ±1.7 to 49.5% ±1.7. This difference is not significant in contrast to the decrease in survival for IPF fibroblasts (p = 0.0004) and normal fibroblasts (p = 0.00007). B) The ability of epithelial cells to survive GSTP1 inhibition is connected to control *GSTP1* mRNA levels (6177 ±1558) more than ten times that of IPF fibroblasts (529 ±182; p = 0.004) or normal fibroblasts (267 ±67; p = 0.001). C) *GSTP1* mRNA levels decline in epithelial cells after both $H_2O_2$ and TLK199/$H_2O_2$ treatment (0.45 fold) with no difference between treatment groups. A decrease (0.45 fold)**

**from the epithelial cell baseline expression score is still five times greater expression of *GSTP1* than IPF fibroblasts. Epithelial cells after TLK199/$H_2O_2$ are still significantly different than IPF fibroblast (p = 0.005) and normal fibroblast (p = 0.035).**

# DISCUSSION

IPF results in a cellular imbalance where there is a significant increase secretory myofibroblasts with and apoptotic resistant phenotype. These myofibroblasts secrete excessive ECM which distorts the lung architecture and may cause the uncontrolled and unexplained decrease in lung epithelium. All lung tissues are exposed to exogenous oxidants and high oxygen levels, but under normal circumstances cells manage this oxidative stress through antioxidant enzyme defense systems including GSH, GST, catalase and superoxide dismutase [9,10].

Oxidative stress is an essential component of the IPF lung environment. Extracellular and intracellular ROS play a critical role in the initiation and the potentiation of lung fibrosis [21,22,24,25]. This study proposed to study the effects of oxidative stress found in the IPF lung environment using an *in vitro* model of IPF and using $H_2O_2$ to simulate oxidative stress.

*Differential Characteristics in IPF and Normal Fibroblasts*

Our initial evaluation of IPF and normal primary fibroblasts found a clear difference in the expression of the following markers of fibroblast activation, *ACTA2* and *COL1A1* (Figure 12) validating our system. Assessment of GST enzyme activity also reveals IPF fibroblasts express more than double the total GST enzyme activity of normal fibroblasts (Figure 10). To determine which of the GST isoforms contribute to this

differential expression, we analyzed the gene expression of each *GST* isoform in both normal and IPF cells. Each *GST* isoform is expressed at a distinct level in each cell line, however no significant difference was observed between IPF and normal fibroblasts in an unstimulated control environment. *GST* isoforms present at minor levels in control lung fibroblasts include *GSTK1*, *GSTT2*, *GSTA4* and *GSTM3* (Figure 8B). In light of our literature review and the known oxidative stress in the IPF lung we expected GSTP1 to be the most abundant GST isoform [28]. Both normal fibroblasts and IPF fibroblasts did, in fact, express more than four times the quantity of GSTP1 than any other GST isoform. The expression score for IPF fibroblasts (529.2 ±182.1) is nearly double that of normal fibroblasts (267.3 ±66.5), indicating its overall importance compared to the other isoforms and its potential as a target for intervention. However, despite this larger expression and the ostensible differential between normal and IPF cells, statistical significance was not achieved. This apparent lack of significance may be explained by the inherent variations observed among primary culture cell lines. In addition, the relatively small sample size may also play into this result. Additional trials and increased sample size may clarify this difference in *GSTP1* expression, as a trend is clear.

*Management of Oxidative Stress in IPF Fibroblasts*

This study reveals an enhanced ability in IPF fibroblasts to cope with the high levels of oxidative stress such as that simulated in the presence of 1 mM $H_2O_2$. In such an oxidative stress environment IPF cells show a significantly greater comparative survival to that of normal fibroblasts (Figure 14). We investigated the potential involvement of GST isoforms in this survival bias by examining the expression of five GST isoforms

exposed to sublethal oxidative stress induced by 200 μM $H_2O_2$. In both cell types, IPF and normal, we found that all isoforms increased their expression. Given the significant survival bias toward IPF fibroblasts, one would expect a significant difference in *GST* isoform expression. We found, however, in an oxidative environment, only *GSTA4* expression showed a significant fold increase in IPF fibroblasts relative to normal fibroblasts (Figure 15).

Interestingly GSTA4 is predominately known for its selective conjugation of GSH to 4-hydroxynonenal (HNE), the most abundant and toxic product of lipid peroxidation [61]. Lipid peroxidation occurs when ROS, including $H_2O_2$, attack unsaturated phospholipids damaging cellular and subcellular membranes [62]. Damage to the mitochondrial membrane leads to release of cytochrome C and induction of apoptosis. GSTA4, because of its selective conjugation of GSH to HNE, provides the main elimination pathway protecting against HNE-mediated cell death and damage [61,63]. HNE also induces expression of *GSTA4* [64]. During the simulated oxidative stress in these experiments IPF fibroblasts showed an increase in their expression of *GSTA4*. This increase of *GSTA4* expression may be pivotal in the general ROS-survival response in IPF. Although GSTA4 is a minor GST isoform in lung fibroblasts, it may afford these cells a better capacity to detoxify HNE, maintain membrane integrity and resist mitochondrial leakage. Further investigation into the role of GSTA4 in IPF fibroblast survival is needed.

Although *GSTP1* gene expression is not significantly increased with 200 μM $H_2O_2$, it is still the predominant GST isoform (Figure 15) and still logically the major

contributor to total GST enzyme activity. GSTP1 activities are not solely associated with conjugation and detoxification. This enzyme makes multiple contributions to other pathways including regulation of nitric oxide, Nuclear Factor kappa β and several kinase signaling pathways [53]. GSTP1 also functions as an inhibitor of c-Jun N-terminal kinase (JNK) through protein-protein interaction and formation of a GSTP1/JNK/c-JUN complex. Formation of this complex inhibits JNK phosphorylation of c-JUN preventing induction of apoptosis or proliferation, dependent on cell type. ROS promote GSTP1 dissociation and oligomerization that permits activation of JNK/c-JUN mediated signaling cascades [44]. Some tumors upregulate GSTP1 increasing JNK sequestration resulting in resistance to drug induced apoptosis [45]. GSTP1 also inhibits JNK activation through regulation of the tumor necrosis factor-α (TNF-α) pathway [45]. Upregulation of TNF- α has been demonstrated in bleomycin- induced pulmonary fibrosis and is associated with activation of Wnt/β- catenin and NF- κB signaling [65]. GSTP1 associates with TRAF2 inhibiting activation of p38-MAPK and JNK. Additionally, GSTP1-TRAF2 inhibits phosphorylation of the activation of TRAF1-enhanced apoptosis signal regulating kinase-1 (ASK-1) and downstream pro-apoptotic signals [45].

In addition to general detoxification of the products of oxidation, GSTP1 assists peroxiredoxins (PRDXs) as they reduce and detoxify $H_2O_2$ [40]. PRDX6 is inactivated after reducing $H_2O_2$. The reactivation of PRDX6 by GSH is complicated by the position of a key residue deep in the structure. Formation of a trimeric complex, PRDX6-GSTP1-GSH, provides a conformational change in PRDX6 that exposes the critical cysteine

residue for regeneration by GSH [39,41]. As a result, GSTP1 is critical for the direct elimination of $H_2O_2$ by PRDX6.

Investigation of the effect of oxidative stress on the cellular levels of total and free GSH found that induced oxidative stress did not result in a change in total and free GSH. This may suggest the function of GSTs, and predominately GSTP1, may be other than conjugation of compounds with GSH.

IPF fibroblasts demonstrate higher total GST enzyme activity under oxidative stress than normal fibroblasts (Figure 16). This activity may be secondary to increased protein synthesis (more enzyme) or from the dissociation from the sequestration by JNK increasing the available GSTP1 pool. Initially, IPF control fibroblasts possess more than double the level of normal control fibroblast GST enzyme activity (Figure 10) and nearly double the *GSTP1* expression score for normal fibroblasts (Figure 8). $H_2O_2$ stress increases IPF total GST activity to nearly four times normal fibroblast GST enzyme activity levels (Figure 16).

ROS and oxidative stress are critical pathogenic factors in the IPF lung environment. While IPF tissue presents a heterogenous population of fibroblasts, the fibroblasts that thrive are those best suited to the oxidative IPF environment [66]. Bocchino, et al, found chronic oxidative stress produced by $H_2O_2$ induced IPF phenotype in control fibroblasts and permitted maintenance of the myofibroblast phenotype [20]. IPF myofibroblasts secrete $H_2O_2$ adding to ROS in the IPF extracellular environment [22]. Higher expression of GSTs and considerably higher GST enzyme activity levels allow

IPF fibroblasts to persist and thrive in the oxidative IPF lung environment exacerbating fibrotic deposition.

*The Critical Role of GSTP is Demonstrated by Inhibition*

The importance of GST to the pathogenesis of IPF was demonstrated by the inhibition of GSTP1, the principal isoform. TLK199 inhibitor exposure directly reduces total GST enzyme activity in IPF fibroblasts by 33% ($p = 0.0489$) (Figure 18). This reduction occurs despite expression increases for other GST isoforms in IPF fibroblast (Figure 19). This apparent contradiction was specific to IPF fibroblasts and may indicate a difference in regulation. IPF fibroblasts appear to rely on the contribution of the GSTP1 isoform as inhibition of this isoform alone is sufficient to greatly reduce total GST enzyme activity. TLK199 eliminates the significant difference in total GST enzyme activity between IPF and normal fibroblasts, essentially normalizing IPF fibroblast behavior. This data implies a differential response in the GST-ROS/survival pathway in IPF fibroblasts that is mitigated by TLK199 resulting in vulnerability to cell death in both IPF and normal fibroblasts.

TLK199 is a GSH peptidomimetic that binds to the G-site of GSTP1 blocking enzymatic repair and detoxification activity as well as altering the site for GSTP1/JNK interaction [52]. TLK199 triggers dissociation of GSTP1 from JNK/c-JUN resulting in activation of the JNK/c-JUN leading to cell death in lung fibroblasts (Figure 24) [44,67]. Inhibition of GSTP1 may also permit TRAF2 activation of p38-MAPK, ASK1 and JNK initiating pro-apoptotic signaling [45].

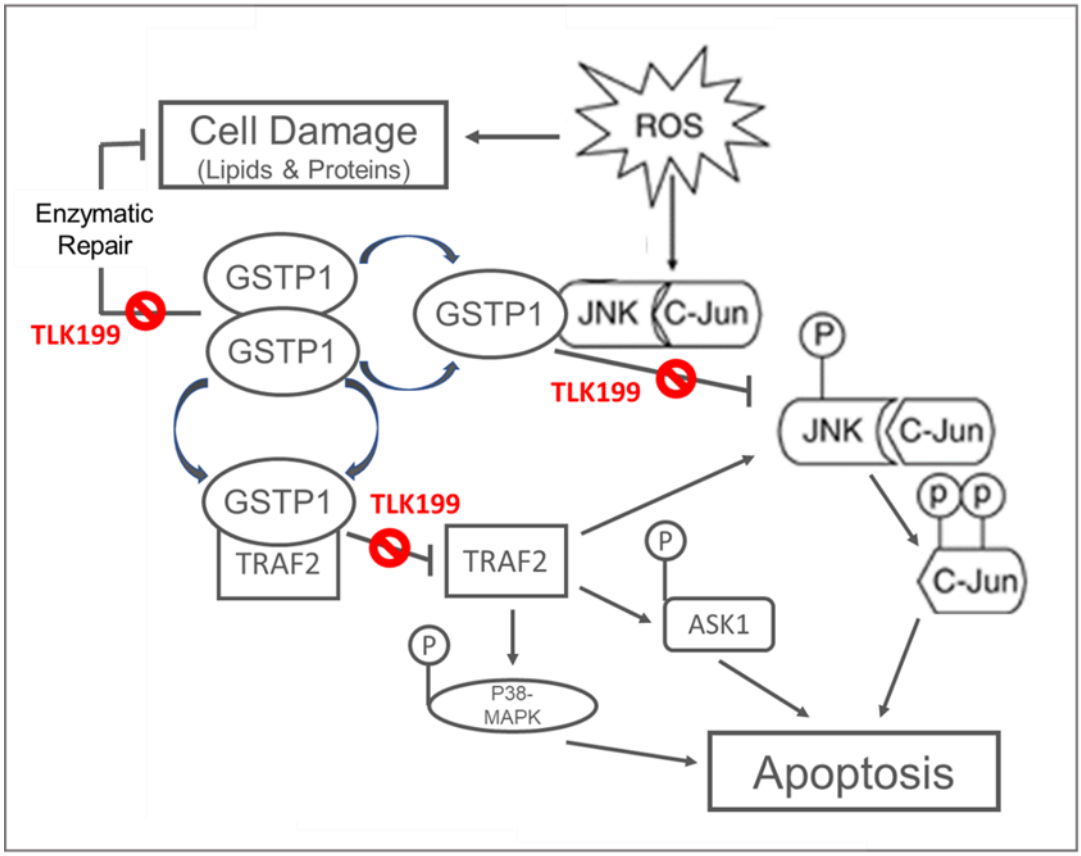


**Figure 24 Putative Action of TLK199 in Lung Fibroblasts.**
**TLK199 inhibits GSTP1 blocking enzymatic repair and detoxification. Inhibition of GSTP1 activates both JNK/c-JUN and TRAF2 signaling pathways leading to apoptosis [44,45].**

Insight into the differential regulation of GST-ROS survival is found in expression of several GST isoforms. GSTP1 inhibition induces increased *GSTP1*, *GSTA4* and *GSTK1* expression in IPF but reduces expression in normal fibroblasts (Figure 19) these alterations are small however not altogether insignificant. As noted GSTA4 eliminates HNE after lipid peroxidation, promoting membrane integrity and impeding apoptosis. Information on GSTK1 is more obscure but there is evidence for the role of GSTK in detoxification of lipid peroxides in both the mitochondrion and peroxisome [68].

This may suggest a synergistic role for GSTA4 in IPF. The IPF specific response upregulating *GSTP1*, *GSTA4* and *GSTK1* may provide an alternate survival mechanism or a more robust response not seen in normal fibroblasts.

Inhibition of GSTP1 significantly reduced survival in both IPF and normal fibroblast cells (Figure 20) however TLK199 inhibition does not result in a reduction in activation of the IPF fibroblast phenotype, as measured by the amount of ACTA2 and COL1A1 (Figure 21). This result is surprising given the familiar role of the GST family, however the dominant function in this situation may be more general protection including inactivation of toxic metabolites of oxidative stress.

Under oxidative stress, there is differential expression of the GST isoforms in IPF fibroblasts compared to normal fibroblasts (Figure 19). Although the process responsible for substantial increases in GST expression in IPF is not examined in this study, the interaction between GSTs and the NRF2-antioxidant response element signaling pathway is documented [50,51]. NRF2 induces phase II antioxidant enzymes through binding to the cis-acting antioxidant response element (ARE) found in the promoter region of numerous protective enzymes including GSTs [69]. NRF2 is highly expressed in the lung where it regulates basal levels of phase II enzymes via interaction with KEAP1 [70]. NRF2 is sequestered in the cytoplasm through association with KEAP1 and routinely targeted for degradation under normal conditions [50,51,70,71]. Oxidative stress results in dissociation of NRF2-KEAP1 and nuclear translocation of NRF2 [50,70]. In the nucleus NRF2 binds to the AREs of target genes in association with cofactors and transcription factors to regulate

transcription [51]. In IPF NRF2 mediation limits bleomycin-induced lung fibrosis and NRF2-null mice reduce ARE associated antioxidant gene expression including GSTs [51].

NRF2 may produce differential regulation in IPF fibroblasts. The direction of NRF2-MAF regulation depends on association with specific transcription factors [51]. NRF2 regulation is also determined by cell type, stimuli or target gene [71,72]. Additionally, a feedforward mechanism has been supported for NRF2 regulation when ROS exceeds a threshold level (Figure 25) [73]. ROS above this critical limit induces Kruppel-like factor 9 (KLF9) resulting in escalation of ROS and consequent cell death. The KLF9 promoter contains ARE3 and ARE4 that have lower binding affinity for NRF2. Unresolved oxidative stress results in the accumulation of nuclear NRF2 making it available for much lower affinity interactions with the KLF9 promoter [73].

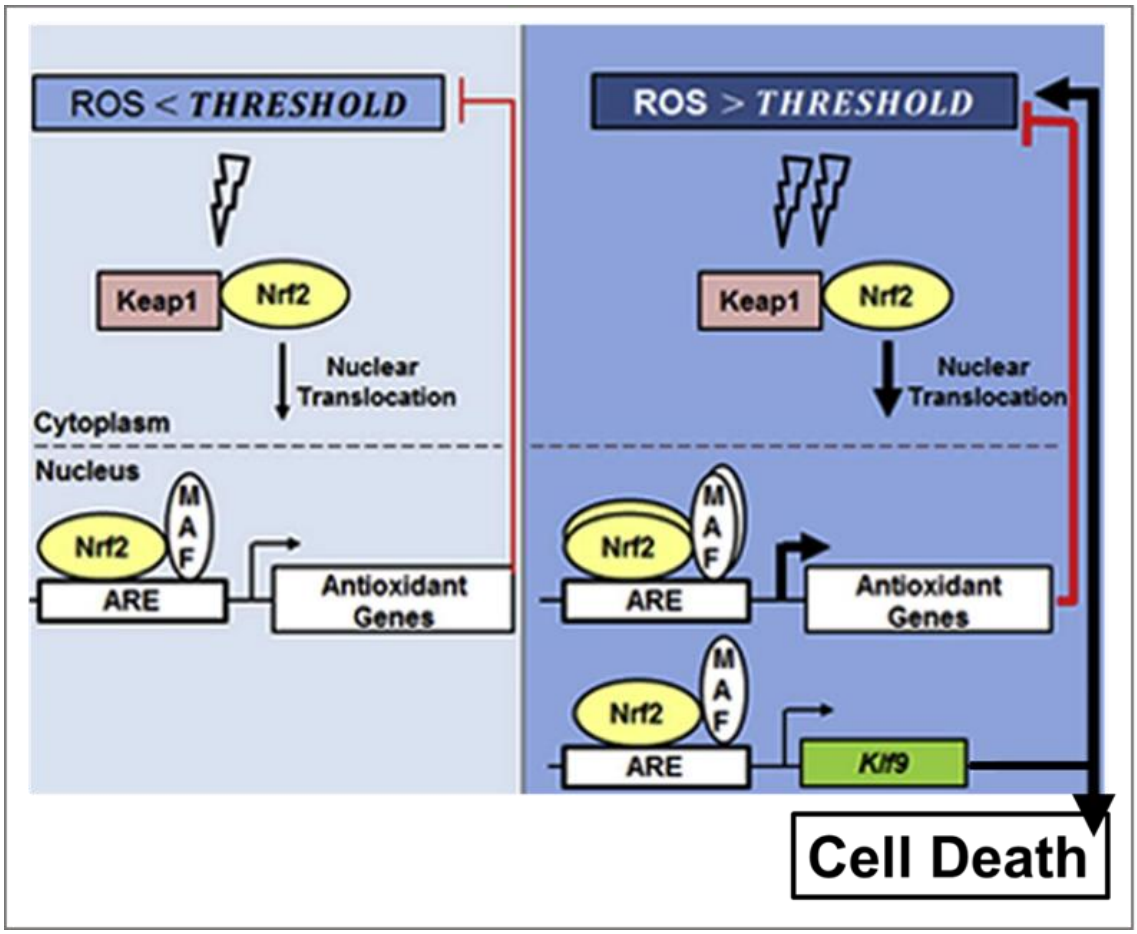


**Figure 25 Potential KLF9-NRF2**
**NRF2 is normally sequestered in the cytoplasm by KEAP1. Oxidative stress results in dissociation and translocation of NRF2 to the nucleus where is binding to ARE inducing transcription of antioxidant genes. Unresolved oxidative stress may lead to accumulation of NRF2 in the nucleus above a threshold that triggers induction of *KLF9* leading to cell death [73].**

NRF2 is specifically elevated in AEC of IPF lung tissue but not in fibroblast foci [74]. Considering the *KLF9* induction threshold, this correlates with survival data after $H_2O_2$ and GSTP inhibition (Figure 20). AEC reduce expression of GSTP under $H_2O_2$ stress. The increased oxidative stress results in dissociation of the abundant NRF2-

KEAP. If nuclear NRF2 accumulates provoking induction of *KLF9*, then reduced survival in AEC would be expected. NRF2 expression is reduced in IPF fibroblasts and linked to apoptosis resistance [75]. The combination of low NRF2 levels and higher expression of *GST* isoforms in IPF fibroblasts may provide resistance to a *KLF9* threshold. Better capacity to manage ROS and a smaller amount of NRF2 available for nuclear translocation may prevent induction of the *KLF9* threshold in IPF fibroblast. Examination of protein levels in the future may identify ROS levels for *KLF9* induction thresholds in normal fibroblasts compared to normal fibroblasts.

## CONCLUSION

Our data indicates a vital role for GST and ROS management in the pathology of IPF. IPF fibroblasts resist ROS induced cell death and demonstrate substantially higher GST enzyme activity than normal fibroblasts as indicated by the activity of the GSTP1 isoform. Low level oxidative stress in IPF fibroblasts results in an upregulation of the isoform *GSTA4*. The subsequent increased ability to metabolize toxic products of lipid peroxidation may facilitate IPF fibroblasts in avoiding apoptosis. The increase in GST expression correlates with superior enzyme activity and increased survival in IPF fibroblasts as compared to normal fibroblasts. Inhibition of the predominate isoform, GSTP1, results in a decline in total GST enzyme activity that normalizes IPF fibroblast enzyme activity to normal fibroblast levels and, more importantly, results in reduced IPF fibroblast survival. Our data indicates blocking GSTP1 mitigates the ability of IPF fibroblasts to evade cell death. The mechanism of this circumvention has yet to be determined.

IPF and normal fibroblasts respond differently to ROS and regulate expression of *GSTP1*, *GSTA4* and *GSTK1* in a disease specific manor. Only IPF fibroblasts increase expression of *GSTP1*, *GSTA4* and *GSTK1* under oxidative stress produced by the inhibition of GSTP1 and the presence of $H_2O_2$. While this upregulation of GSTs does not compensate for the loss of total enzyme activity due to GSTP inhibition, it is evidence for

IPF differential response and regulation. The role of JNK/c-JUN as well as NRF2-ARE regulation of *GSTP1*, *GSTA4* and *GSTK1* in IPF remains to be elucidated.

## Future Directions

Increases in *GSTA4* and *GSTK1* mRNA levels correlate to increased survival in IPF, but it is not known if these isoforms are regulated in a manner comparable to *GSTP1*. *GSTA4* was upregulated by low level ROS alone as well as GSTP inhibitor, while *GSTK1* significantly increased only with TLK199/$H_2O_2$. Relative contributions of these isoforms could be determined by inhibitors with isoform specificity. The TLK199 inhibitor used for this study has high specificity for GSTP1. Since IPF fibroblasts use multiple GST isoforms to manage increasing oxidative stress, investigation of inhibitors with less specificity or a combination of GSTP and GSTA inhibitors may increase efficacy and reduce IPF fibroblast survival.

The role of NRF2-ARE transcriptional regulation in IPF remains to be examined. As seen in *KLF9* induction, variations in ARE binding affinity may play a role in the disease specific regulation of *GSTA4* and *GSTK1*. This may begin with *in silico* analysis of upstream and downstream regions of these genes for ARE variations. Exploration of different NRF2-KLF9 thresholds in IPF fibroblasts compared to normal fibroblasts would inform our understanding of fibrosis related survival and cell death. We propose examination of ROS activation of NRF2 and NRF2 localization to the nucleus as compared to *KLF9* expression to identify a potential NRF2-KLF9 threshold.

Confirmation of the NRF2-KLF9 threshold could be obtained by over-expression of NRF2.

Further analysis of protein levels in IPF and normal fibroblasts would inform our understanding of the role of GSTP1 in cell signaling. Comparison of activated c-JUN with and without GSTP1 inhibitor as well as other biomarkers for intrinsic apoptosis would help define the mechanism of cell death induced by GSTP1 inhibition. Our findings establish a key role for GSTs in IPF fibroblast cell survival. Further elucidation of the mechanisms connecting regulation of GSTs and pathways regulating apoptosis are essential for improved treatment and outcomes for patients suffering from IPF.

# APPENDIX

## Appendix A

### Data Analysis: Hydrogen Peroxide Toxicity

Descriptive Statistics: Percent Survival
Results for H2O2 (uM) = 200
Statistics

| Variable | Cell Type | N | N* | Mean | SE Mean | StDev | Minimum | Q1 | Median | Q3 | Maximum |
|---|---|---|---|---|---|---|---|---|---|---|---|
| Percent Survival | IPF | 2 | 0 | 105.7 | 15.4 | 21.8 | 90.2 | * | 105.7 | * | 121.1 |
| | Normal | 2 | 0 | 110.6 | 13.9 | 19.6 | 96.7 | * | 110.6 | * | 124.4 |

Results for H2O2 (uM) = 800
Statistics

| Variable | Cell Type | N | N* | Mean | SE Mean | StDev | Minimum | Q1 | Median | Q3 | Maximum |
|---|---|---|---|---|---|---|---|---|---|---|---|
| Percent Survival | IPF | 2 | 0 | 77.0 | 13.9 | 19.7 | 63.1 | * | 77.0 | * | 90.9 |
| | Normal | 2 | 0 | 96.60 | 6.70 | 9.48 | 89.90 | * | 96.60 | * | 103.30 |

Results for H2O2 (uM) = 1000
Statistics

| Variable | Cell Type | N | N* | Mean | SE Mean | StDev | Minimum | Q1 | Median | Q3 | Maximum |
|---|---|---|---|---|---|---|---|---|---|---|---|
| Percent Survival | IPF | 2 | 0 | 51.80 | 3.00 | 4.24 | 48.80 | * | 51.80 | * | 54.80 |
| | Normal | 2 | 0 | 55.1 | 25.9 | 36.6 | 29.2 | * | 55.1 | * | 81.0 |

One-way ANOVA: Hydrogen Peroxide Toxicity Analysis

Method

| | |
|---|---|
| Null hypothesis | All means are equal |
| Alternative hypothesis | Not all means are equal |
| Significance level | $\alpha = 0.05$ |

*Equal variances were assumed for the analysis.*

Factor Information

| Factor | Levels | Values |
|---|---|---|
| Factor | 4 | 0, 200, 800, 1000 |

Analysis of Variance

| Source | DF | Adj SS | Adj MS | F-Value | P-Value |
|---|---|---|---|---|---|
| Factor | 3 | 8645 | 2881.6 | 14.09 | 0.000 |
| Error | 20 | 4089 | 204.4 | | |
| Total | 23 | 12734 | | | |

Model Summary

| S | R-sq | R-sq(adj) | R-sq(pred) |
|---|---|---|---|
| 14.2986 | 67.89% | 63.07% | 53.76% |

Means

| Factor | N | Mean | StDev | 95% CI |
|---|---|---|---|---|
| 0 | 6 | 100.0 | 0.0 | (87.8, 112.2) |
| 200 | 6 | 106.32 | 17.00 | (94.14, 118.49) |
| 800 | 6 | 86.37 | 14.72 | (74.19, 98.54) |
| 1000 | 6 | 57.02 | 17.67 | (44.84, 69.19) |

*Pooled StDev = 14.2986*

Tukey Pairwise Comparisons

Grouping Information Using the Tukey Method and 95% Confidence

| Factor | N | Mean | Grouping |
|---|---|---|---|
| 200 | 6 | 106.32 | A |
| 0 | 6 | 100.0 | A |
| 800 | 6 | 86.37 | A |
| 1000 | 6 | 57.02 | B |

*Means that do not share a letter are significantly different.*

Fisher Pairwise Comparisons

Grouping Information Using the Fisher LSD Method and 95% Confidence

| Factor | N | Mean | Grouping | | |
|---|---|---|---|---|---|
| 200 | 6 | 106.32 | A | | |
| 0 | 6 | 100.0 | A | B | |
| 800 | 6 | 86.37 | | B | |
| 1000 | 6 | 57.02 | | | C |

*Means that do not share a letter are significantly different.*

One-Sample T: 200 μM $H_2O_2$

Descriptive Statistics

| N | Mean | StDev | SE Mean | 95% CI for μ |
|---|---|---|---|---|
| 6 | 106.32 | 17.00 | 6.94 | (88.48, 124.16) |

*μ: mean of 200*

Test

Null hypothesis $H_0 : \mu = 100$

Alternative hypothesis $H_1 : \mu \neq 100$

| T-Value | P-Value |
|---|---|
| 0.91 | 0.404 |

One-Sample T: 1000 μM $H_2O_2$

Descriptive Statistics

| N | Mean | StDev | SE Mean | 95% CI for μ |
|---|---|---|---|---|
| 6 | 57.02 | 17.67 | 7.21 | (38.47, 75.56) |

*μ: mean of 1000*

Test

Null hypothesis $H_0 : \mu = 100$

Alternative hypothesis $H_1 : \mu \neq 100$

| T-Value | P-Value |
|---|---|
| -5.96 | 0.002 |

## Appendix B

### qPCR Expression Score formula for Control Cells mRNA Levels

| *GSTA4* | *GSTK1* | *GSTM3* | *GSTP1* | *GSTT2* | *ACTA2* | *COL1A1* |
|---|---|---|---|---|---|---|
| $1x10^5/2^{\Delta CT}$ | $1x10^5/2^{\Delta CT}$ | $1x10^5/2^{\Delta CT}$ | $1x10^5/2^{\Delta CT}$ | $1x10^5/2^{\Delta CT}$ | $5x10^4/2^{\Delta CT}$ | $1x10^3/2^{\Delta CT}$ |

| | Expression Score | | | | | | |
|---|---|---|---|---|---|---|---|
| | GSTA4 | GSTK1 | GSTM3 | GSTP1 | GSTT2 | ACTA 2 | COL1A1 |
| GLN113 | 3.3 | 110.7 | 1.2 | 491.3 | 31.6 | 11.7 | 11.5 |
| N2 | 1.3 | 50.5 | 1.9 | 224.0 | 1.7 | 13.6 | 4.6 |
| N4 | 2.5 | 48.9 | 1.5 | 210.5 | 40.1 | 58.7 | 8.9 |
| N7 | 1.6 | 47.9 | 0.8 | 143.3 | 5.6 | 22.2 | 5.7 |
| GLN113 H2O2 | 5.8 | 197.9 | 1.8 | 676.6 | 46.7 | 22.5 | 11.5 |
| N2 H2O2 | 2.3 | 82.3 | 4.3 | 424.3 | 3.8 | 18.8 | 5.0 |
| N4 H2O2 | 1.9 | 40.2 | 1.7 | 162.7 | 33.4 | 41.6 | 6.2 |
| N7 H2O2 | 1.5 | 36.5 | 1.0 | 92.4 | 14.3 | 14.0 | 6.5 |
| GLN 113 INH | 2.5 | 100.2 | 1.0 | 381.9 | 22.8 | 12.2 | 10.7 |
| N2 INH | 1.7 | 52.8 | 3.6 | 327.5 | 3.1 | 11.4 | 2.5 |
| N4 INH | 0.8 | 23.9 | 0.8 | 84.4 | 8.8 | 26.8 | 3.3 |
| N7 INH | 1.4 | 54.7 | 1.6 | 157.9 | 16.0 | 13.4 | 5.4 |
| IPF330 | 2.8 | 71.0 | 3.3 | 331.5 | 19.6 | 59.6 | 38.2 |
| IPF018 | 2.0 | 69.7 | 1.2 | 323.8 | 14.6 | 82.5 | 18.1 |
| IPF019 | 4.1 | 73.3 | 1.6 | 301.6 | 18.0 | 103.2 | 15.7 |
| IPF335 | 11.0 | 167.3 | 2.7 | 1159.8 | 6.8 | 282.7 | 127.3 |
| IPF330 H2O2 | 7.6 | 108.0 | 5.8 | 566.3 | 31.9 | 85.8 | 37.1 |
| IPF018 H2O2 | 2.9 | 72.8 | 1.4 | 355.1 | 15.0 | 69.2 | 16.0 |
| IPF019 H2O2 | 8.4 | 128.0 | 2.3 | 532.4 | 21.4 | 143.3 | 20.3 |
| IPF335 H2O2 | 14.8 | 127.7 | 3.1 | 788.5 | 5.1 | 234.4 | 110.3 |
| IPF330 INH | 6.5 | 108.7 | 4.1 | 535.2 | 36.0 | 82.2 | 52.5 |
| IPF018 INH | 7.4 | 193.5 | 3.7 | 657.0 | 31.8 | 150.8 | 30.2 |
| IPF019 INH | 4.7 | 86.6 | 1.3 | 267.4 | 17.5 | 103.5 | 18.9 |
| IPF335 INH | 8.8 | 148.0 | 2.5 | 1481.6 | 11.1 | 238.8 | 68.1 |
| A549 | 18.5 | 289.3 | 1.6 | 8381.4 | 1.3 | 5.6 | 0.1 |
| HSAEC | 9.8 | 231.7 | 3.4 | 3973.8 | 4.4 | 32.1 | 0.1 |
| A549 H2O2 | 9.1 | 174.4 | 0.7 | 2689.2 | 0.5 | 5.7 | 0.1 |
| HSAEC H2O2 | 7.1 | 181.8 | 1.6 | 2298.2 | 2.3 | 19.4 | 0.0 |
| A549 INH | 8.7 | 125.9 | 0.7 | 1973.2 | 0.6 | 5.1 | 0.1 |
| HSAEC INH | 7.4 | 205.0 | 2.2 | 2640.0 | 3.0 | 21.5 | 0.0 |

## Appendix C

### Analysis of Survival Data IPF vs Normal Fibroblasts

One-way ANOVA: Data for Survival IPF vs Normal Fibroblasts Method

| | |
|---|---|
| Null hypothesis | All means are equal |
| Alternative hypothesis | Not all means are equal |
| Significance level | $\alpha = 0.05$ |

*Equal variances were assumed for the analysis.*

Factor Information

| Factor | Levels | Values |
|---|---|---|
| Cell Type | 2 | IPF, Normal |

Analysis of Variance

| Source | DF | Adj SS | Adj MS | F-Value | P-Value |
|---|---|---|---|---|---|
| Cell Type | 1 | 573.2 | 573.2 | 5.50 | 0.031 |
| Error | 17 | 1770.0 | 104.1 | | |
| Total | 18 | 2343.2 | | | |

Model Summary

| S | R-sq | R-sq(adj) | R-sq(pred) |
|---|---|---|---|
| 10.2038 | 24.46% | 20.02% | 5.77% |

Means

| Cell Type | N | Mean | StDev | 95% CI |
|---|---|---|---|---|
| IPF | 10 | 74.00 | 10.73 | (67.19, 80.81) |
| Normal | 9 | 63.00 | 9.58 | (55.82, 70.18) |

*Pooled StDev = 10.2038*

Tukey Pairwise Comparisons

Grouping Information Using the Tukey Method and 95% Confidence

| Cell Type | N | Mean | Grouping |
|---|---|---|---|
| IPF | 10 | 74.00 | A |
| Normal | 9 | 63.00 | B |

*Means that do not share a letter are significantly different.*

Tukey Simultaneous 95% CIs

Fisher Pairwise Comparisons

Grouping Information Using the Fisher LSD Method and 95% Confidence

| Cell Type | N | Mean | Grouping | |
|---|---|---|---|---|
| IPF | 10 | 74.00 | A | |
| Normal | 9 | 63.00 | | B |

*Means that do not share a letter are significantly different.*

## Appendix D

### Data Analysis: TLK199 Toxicity

One-way ANOVA: TLK199 Concentrations 0, 25, 50, and 100 uM for Toxicity Analysis

#### Method

| | |
|---|---|
| Null hypothesis | All means are equal |
| Alternative hypothesis | Not all means are equal |
| Significance level | $\alpha = 0.05$ |

*Equal variances were assumed for the analysis.*

#### Factor Information

| Factor | Levels | Values |
|---|---|---|
| Factor | 4 | 0, 25, 50, 100 |

#### Analysis of Variance

| Source | DF | Adj SS | Adj MS | F-Value | P-Value |
|---|---|---|---|---|---|
| Factor | 3 | 7353 | 2450.9 | 19.40 | 0.000 |
| Error | 20 | 2527 | 126.4 | | |
| Total | 23 | 9880 | | | |

#### Model Summary

| S | R-sq | R-sq(adj) | R-sq(pred) |
|---|---|---|---|
| 11.2407 | 74.42% | 70.58% | 63.17% |

#### Means

| Factor | N | Mean | StDev | 95% CI |
|---|---|---|---|---|
| 0 | 6 | 100.0 | 0.0 | (90.4, 109.6) |
| 25 | 6 | 97.08 | 7.82 | (87.51, 106.66) |
| 50 | 6 | 86.93 | 8.97 | (77.36, 96.51) |
| 100 | 6 | 55.83 | 19.07 | (46.26, 65.41) |

*Pooled StDev = 11.2407*

Tukey Pairwise Comparisons

#### Grouping Information Using the Tukey Method and 95% Confidence

| Factor | N | Mean | Grouping |
|---|---|---|---|
| 0 | 6 | 100.0 | A |
| 25 | 6 | 97.08 | A |

| | | | |
|---|---|---|---|
| 50 | 6 | 86.93 | A |
| 100 | 6 | 55.83 | B |

*Means that do not share a letter are significantly different.*

## Tukey Simultaneous Tests for Differences of Means

| Difference of Levels | Difference of Means | SE of Difference | 95% CI | T-Value | Adjusted P-Value |
|---|---|---|---|---|---|
| 25 - 0 | -2.92 | 6.49 | (-21.09, 15.26) | -0.45 | 0.969 |
| 50 - 0 | -13.07 | 6.49 | (-31.24, 5.11) | -2.01 | 0.216 |
| 100 - 0 | -44.17 | 6.49 | (-62.34, -25.99) | -6.81 | 0.000 |
| 50 - 25 | -10.15 | 6.49 | (-28.32, 8.02) | -1.56 | 0.420 |
| 100 - 25 | -41.25 | 6.49 | (-59.42, -23.08) | -6.36 | 0.000 |
| 100 - 50 | -31.10 | 6.49 | (-49.27, -12.93) | -4.79 | 0.001 |

*Individual confidence level = 98.89%*

## Fisher Pairwise Comparisons

Grouping Information Using the Fisher LSD Method and 95% Confidence

| Factor | N | Mean | Grouping |
|---|---|---|---|
| 0 | 6 | 100.0 | A |
| 25 | 6 | 97.08 | A |
| 50 | 6 | 86.93 | A |
| 100 | 6 | 55.83 | B |

*Means that do not share a letter are significantly different.*

## Fisher Individual Tests for Differences of Means

| Difference of Levels | Difference of Means | SE of Difference | 95% CI | T-Value | Adjusted P-Value |
|---|---|---|---|---|---|
| 25 - 0 | -2.92 | 6.49 | (-16.45, 10.62) | -0.45 | 0.658 |
| 50 - 0 | -13.07 | 6.49 | (-26.60, 0.47) | -2.01 | 0.058 |
| 100 - 0 | -44.17 | 6.49 | (-57.70, -30.63) | -6.81 | 0.000 |
| 50 - 25 | -10.15 | 6.49 | (-23.69, 3.39) | -1.56 | 0.134 |
| 100 - 25 | -41.25 | 6.49 | (-54.79, -27.71) | -6.36 | 0.000 |
| 100 - 50 | -31.10 | 6.49 | (-44.64, -17.56) | -4.79 | 0.000 |

*Simultaneous confidence level = 80.83%*

## Appendix E

### Analysis of Survival with TLK199 Pre-treatment

One-way ANOVA: Survival by Cell Type with TLK199 Pre-treatment

Method

| | |
|---|---|
| Null hypothesis | All means are equal |
| Alternative hypothesis | Not all means are equal |
| Significance level | $\alpha = 0.05$ |

*Equal variances were assumed for the analysis.*

Factor Information

| Factor | Levels | Values |
|---|---|---|
| Cell Type | 3 | Epithelial, IPF, Normal |

Analysis of Variance

| Source | DF | Adj SS | Adj MS | F-Value | P-Value |
|---|---|---|---|---|---|
| Cell Type | 2 | 2125 | 1062.3 | 3.19 | 0.104 |
| Error | 7 | 2335 | 333.5 | | |
| Total | 9 | 4459 | | | |

Model Summary

| S | R-sq | R-sq(adj) | R-sq(pred) |
|---|---|---|---|
| 18.2623 | 47.64% | 32.69% | 6.30% |

Means

| Cell Type | N | Mean | StDev | 95% CI |
|---|---|---|---|---|
| Epithelial | 2 | 49.50 | 3.54 | (18.96, 80.04) |
| IPF | 4 | 40.59 | 17.04 | (19.00, 62.18) |
| Normal | 4 | 14.6 | 22.0 | (-7.0, 36.1) |

*Pooled StDev = 18.2623*

Tukey Pairwise Comparisons

Grouping Information Using the Tukey Method and 95% Confidence

| Cell Type | N | Mean | Grouping |
|---|---|---|---|
| Epithelial | 2 | 49.50 | A |

| | | | |
|---|---|---|---|
| IPF | 4 | 40.59 | A |
| Normal | 4 | 14.6 | A |

*Means that do not share a letter are significantly different.*

Tukey Simultaneous 95% CIs
Fisher Pairwise Comparisons
Grouping Information Using the Fisher LSD Method and 95% Confidence

| Cell Type | N | Mean | Grouping |
|---|---|---|---|
| Epithelial | 2 | 49.50 | A |
| IPF | 4 | 40.59 | A |
| Normal | 4 | 14.6 | A |

*Means that do not share a letter are significantly different.*

# Appendix F

## qPCR Expression Data $H_2O_2$ and TLK199/$H_2O_2$

| | Delta | | | | | | | Delta/Delta | | | | | | |
|---|---|---|---|---|---|---|---|---|---|---|---|---|---|---|
| | GSTA4 | GSTK1 | GSTM3 | GSTP1 | GSTT2 | ACTA 2 | COL1A1 | GSTA4 | GSTK1 | GSTM3 | GSTP1 | GSTT2 | ACTA 2 | COL1A1 |
| GLN113 | 14.9 | 9.8 | 16.4 | 7.7 | 11.6 | 12.1 | 6.4 | 0.0 | 0.0 | 0.0 | 0.0 | 0.0 | 0.0 | 0.0 |
| N2 | 16.3 | 11.0 | 15.7 | 8.8 | 15.9 | 11.8 | 7.8 | 0.0 | 0.0 | 0.0 | 0.0 | 0.0 | 0.0 | 0.0 |
| N4 | 15.3 | 11.0 | 16.0 | 8.9 | 11.3 | 9.7 | 6.8 | 0.0 | 0.0 | 0.0 | 0.0 | 0.0 | 0.0 | 0.0 |
| N7 | 16.0 | 11.0 | 16.9 | 9.4 | 14.1 | 11.1 | 7.5 | 0.0 | 0.0 | 0.0 | 0.0 | 0.0 | 0.0 | 0.0 |
| GLN113 H2O2 | 14.1 | 9.0 | 15.8 | 7.2 | 11.1 | 11.1 | 6.4 | 0.8 | 0.8 | 0.6 | 0.5 | 0.6 | 0.9 | 0.0 |
| N2 H2O2 | 15.4 | 10.2 | 14.5 | 7.9 | 14.7 | 11.4 | 7.6 | 0.9 | 0.7 | 1.1 | 0.9 | 1.2 | 0.5 | 0.1 |
| N4 H2O2 | 15.7 | 11.3 | 15.9 | 9.3 | 11.5 | 10.2 | 7.3 | -0.4 | -0.3 | 0.1 | -0.4 | -0.3 | -0.5 | -0.5 |
| N7 H2O2 | 16.0 | 11.4 | 16.6 | 10.1 | 12.8 | 11.8 | 7.3 | 0.0 | -0.4 | 0.3 | -0.6 | 1.4 | -0.7 | 0.2 |
| GLN 113 INH | 15.3 | 10.0 | 16.6 | 8.0 | 12.1 | 12.0 | 6.5 | -0.4 | -0.1 | -0.3 | -0.4 | -0.5 | 0.1 | -0.1 |
| N2 INH | 15.9 | 10.9 | 14.7 | 8.3 | 15.0 | 12.1 | 8.6 | 0.4 | 0.1 | 0.9 | 0.5 | 0.9 | -0.3 | -0.9 |
| N4 INH | 17.0 | 12.0 | 17.0 | 10.2 | 13.5 | 10.9 | 8.2 | -1.7 | -1.0 | -1.0 | -1.3 | -2.2 | -1.1 | -1.4 |
| N7 INH | 16.1 | 10.8 | 16.0 | 9.3 | 12.6 | 11.9 | 7.5 | -0.1 | 0.2 | 0.9 | 0.1 | 1.5 | -0.7 | -0.1 |
| IPF330 | 15.1 | 10.5 | 14.9 | 8.2 | 12.3 | 9.7 | 4.7 | 0.0 | 0.0 | 0.0 | 0.0 | 0.0 | 0.0 | 0.0 |
| IPF018 | 15.6 | 10.5 | 16.4 | 8.3 | 12.7 | 9.2 | 5.8 | 0.0 | 0.0 | 0.0 | 0.0 | 0.0 | 0.0 | 0.0 |
| IPF019 | 14.6 | 10.4 | 16.0 | 8.4 | 12.4 | 8.9 | 6.0 | 0.0 | 0.0 | 0.0 | 0.0 | 0.0 | 0.0 | 0.0 |
| IPF335 | 13.1 | 9.2 | 15.2 | 6.4 | 13.8 | 7.5 | 3.0 | 0.0 | 0.0 | 0.0 | 0.0 | 0.0 | 0.0 | 0.0 |
| IPF330 H2O2 | 13.7 | 9.9 | 14.1 | 7.5 | 11.6 | 9.2 | 4.8 | 1.4 | 0.6 | 0.8 | 0.8 | 0.7 | 0.5 | 0.0 |
| IPF018 H2O2 | 15.1 | 10.4 | 16.2 | 8.1 | 12.7 | 9.5 | 6.0 | 0.5 | 0.1 | 0.2 | 0.1 | 0.0 | -0.3 | -0.2 |
| IPF019 H2O2 | 13.5 | 9.6 | 15.4 | 7.6 | 12.2 | 8.4 | 5.6 | 1.0 | 0.8 | 0.6 | 0.8 | 0.2 | 0.5 | 0.4 |
| IPF335 H2O2 | 12.7 | 9.6 | 15.0 | 7.0 | 14.2 | 7.7 | 3.2 | 0.4 | -0.4 | 0.2 | -0.6 | -0.4 | -0.3 | -0.2 |
| IPF330 INH | 13.9 | 9.8 | 14.6 | 7.5 | 11.4 | 9.2 | 4.3 | 1.2 | 0.6 | 0.3 | 0.7 | 0.9 | 0.5 | 0.5 |
| IPF018 INH | 13.7 | 9.0 | 14.7 | 7.3 | 11.6 | 8.4 | 5.1 | 1.9 | 1.5 | 1.6 | 1.0 | 1.1 | 0.9 | 0.7 |
| IPF019 INH | 14.4 | 10.2 | 16.2 | 8.5 | 12.5 | 8.9 | 5.7 | 0.2 | 0.2 | -0.2 | -0.2 | 0.0 | 0.0 | 0.3 |
| IPF335 INH | 13.5 | 9.4 | 15.3 | 6.1 | 13.1 | 7.7 | 3.9 | -0.3 | -0.2 | -0.1 | 0.4 | 0.7 | -0.2 | -0.9 |
| A549 | 12.4 | 8.4 | 15.9 | 3.6 | 16.2 | 13.1 | 12.8 | 0.0 | 0.0 | 0.0 | 0.0 | 0.0 | 0.0 | 0.0 |
| HSAEC | 13.3 | 8.8 | 14.8 | 4.7 | 14.5 | 10.6 | 13.4 | 0.0 | 0.0 | 0.0 | 0.0 | 0.0 | 0.0 | 0.0 |
| A549 H2O2 | 13.4 | 9.2 | 17.1 | 5.2 | 17.7 | 13.1 | 13.8 | -1.0 | -0.7 | -1.2 | -1.6 | -1.5 | 0.0 | -1.0 |
| HSAEC H2O2 | 13.8 | 9.1 | 15.9 | 5.4 | 15.4 | 11.3 | 15.1 | -0.5 | -0.4 | -1.1 | -0.8 | -0.9 | -0.7 | -1.7 |
| A549 INH | 13.5 | 9.6 | 17.1 | 5.7 | 17.4 | 13.3 | 13.5 | -1.1 | -1.2 | -1.2 | -2.1 | -1.2 | -0.1 | -0.8 |
| HSAEC INH | 13.7 | 8.9 | 15.5 | 5.2 | 15.0 | 11.2 | 14.5 | -0.4 | -0.2 | -0.7 | -0.6 | -0.6 | -0.6 | -1.2 |

## Appendix G

## Glutathione Assay Analysis

Repeated Measures ANOVA

Within Subjects Effects

| | Sum of Squares | df | Mean Square | F | p |
|---|---|---|---|---|---|
| RM Factor 1 | 96.3 | 2 | 48.1 | 3.28 | 0.091 |
| RM Factor 1 ✻ Disease | 34.9 | 2 | 17.5 | 1.19 | 0.353 |
| Residual | 117.5 | 8 | 14.7 | | |

Note. Type 3 Sums of Squares

Between Subjects Effects

| | Sum of Squares | df | Mean Square | F | p |
|---|---|---|---|---|---|
| Disease | 22.9 | 1 | 22.9 | 0.446 | 0.541 |
| Residual | 205.2 | 4 | 51.3 | | |

Note. Type 3 Sums of Squares

Post Hoc Tests

Post Hoc Comparisons - RM Factor 1 ✻ Disease

| Comparison | | | | | | | | | | | | | |
|---|---|---|---|---|---|---|---|---|---|---|---|---|---|
| RM Factor | Disease | | RM Factor 1 | Disease | Mean | SE | df | t | p | ptukey | pscheffe | pbonferron | pholm |
| Untreated | IPF | - | Untreated | Normal | -0.901 | 4.23 | 8.5 | -0.213 | 0.837 | 1 | 1 | 1.0000 | 1 |
| | | - | H202 | IPF | -3.241 | 3.13 | 8 | -1.036 | 0.331 | 0.893 | 0.947 | 1.0000 | 1 |
| | | - | H202 | Normal | 2.635 | 4.23 | 8.5 | 0.622 | 0.55 | 0.986 | 0.994 | 1.0000 | 1 |
| | | - | TLK | IPF | -6.174 | 3.13 | 8 | -1.973 | 0.084 | 0.429 | 0.592 | 1.0000 | 1 |
| | | - | TLK | Normal | -4.387 | 4.23 | 8.5 | -1.036 | 0.329 | 0.894 | 0.947 | 1.0000 | 1 |
| | Normal | - | H202 | IPF | -2.34 | 4.23 | 8.5 | -0.553 | 0.595 | 0.992 | 0.997 | 1.0000 | 1 |
| | | - | H202 | Normal | 3.536 | 3.13 | 8 | 1.13 | 0.291 | 0.856 | 0.925 | 1.0000 | 1 |
| | | - | TLK | IPF | -5.273 | 4.23 | 8.5 | -1.245 | 0.246 | 0.805 | 0.894 | 1.0000 | 1 |
| | | - | TLK | Normal | -3.487 | 3.13 | 8 | -1.114 | 0.297 | 0.863 | 0.929 | 1.0000 | 1 |
| H202 | IPF | - | H202 | Normal | 5.876 | 4.23 | 8.5 | 1.388 | 0.201 | 0.734 | 0.846 | 1.0000 | 1 |
| | | - | TLK | IPF | -2.933 | 3.13 | 8 | -0.937 | 0.376 | 0.925 | 0.964 | 1.0000 | 1 |
| | | - | TLK | Normal | -1.147 | 4.23 | 8.5 | -0.271 | 0.793 | 1 | 1 | 1.0000 | 1 |
| | Normal | - | TLK | IPF | -8.809 | 4.23 | 8.5 | -2.081 | 0.069 | 0.376 | 0.541 | 1.0000 | 0.966 |
| | | - | TLK | Normal | -7.023 | 3.13 | 8 | -2.244 | 0.055 | 0.314 | 0.471 | 0.8260 | 0.826 |
| TLK | IPF | - | TLK | Normal | 1.787 | 4.23 | 8.5 | 0.422 | 0.684 | 0.998 | 0.999 | 1.0000 | 1 |

## Appendix H

### Glutathione Transferase Activity Assay

One-way ANOVA: GST Concentration versus Treatment Method

| | |
|---|---|
| Null hypothesis | All means are equal |
| Alternative hypothesis | Not all means are equal |
| Significance level | $\alpha = 0.05$ |
| Rows unused | 1 |

*Equal variances were assumed for the analysis.*

Factor Information

| Factor | Levels | Values |
|---|---|---|
| Treatment | 6 | IPF H2O2, IPF Media, IPF TLK, Norm H2O2, Norm Media, Norm TLK |

Analysis of Variance

| Source | DF | Adj SS | Adj MS | F-Value | P-Value |
|---|---|---|---|---|---|
| Treatment | 5 | 11458 | 2291.6 | 11.71 | 0.000 |
| Error | 47 | 9201 | 195.8 | | |
| Total | 52 | 20659 | | | |

Model Summary

| S | R-sq | R-sq(adj) | R-sq(pred) |
|---|---|---|---|
| 13.9914 | 55.46% | 50.73% | 42.73% |

Means

| Treatment | N | Mean | StDev | 95% CI |
|---|---|---|---|---|
| IPF H2O2 | 8 | 54.96 | 25.71 | (45.01, 64.91) |
| IPF Media | 9 | 49.67 | 9.74 | (40.29, 59.06) |
| IPF TLK | 9 | 39.25 | 7.14 | (29.86, 48.63) |
| Norm H2O2 | 9 | 15.11 | 6.68 | (5.73, 24.50) |
| Norm Media | 9 | 19.50 | 7.71 | (10.12, 28.88) |
| Norm TLK | 9 | 27.48 | 17.94 | (18.09, 36.86) |

*Pooled StDev = 13.9914*

Tukey Pairwise Comparisons

Grouping Information Using the Tukey Method and 95% Confidence

| Treatment | N | Mean | Grouping | | |
|---|---|---|---|---|---|
| IPF H2O2 | 8 | 54.96 | A | | |
| IPF Media | 9 | 49.67 | A | | |
| IPF TLK | 9 | 39.25 | A | B | |
| Norm TLK | 9 | 27.48 | | B | C |
| Norm Media | 9 | 19.50 | | | C |
| Norm H2O2 | 9 | 15.11 | | | C |

*Means that do not share a letter are significantly different.*

## Tukey Simultaneous Tests for Differences of Means

| Difference of Levels | Difference of Means | SE of Difference | 95% CI | T-Value | Adjusted P-Value |
|---|---|---|---|---|---|
| IPF Media - IPF H2O2 | -5.29 | 6.80 | (-25.48, 14.90) | -0.78 | 0.970 |
| IPF TLK - IPF H2O2 | -15.72 | 6.80 | (-35.91, 4.48) | -2.31 | 0.210 |
| Norm H2O2 - IPF H2O2 | -39.85 | 6.80 | (-60.04, -19.66) | -5.86 | 0.000 |
| Norm Media - IPF H2O2 | -35.46 | 6.80 | (-55.65, -15.27) | -5.22 | 0.000 |
| Norm TLK - IPF H2O2 | -27.48 | 6.80 | (-47.68, -7.29) | -4.04 | 0.003 |
| IPF TLK - IPF Media | -10.43 | 6.60 | (-30.02, 9.16) | -1.58 | 0.615 |
| Norm H2O2 - IPF Media | -34.56 | 6.60 | (-54.15, -14.97) | -5.24 | 0.000 |
| Norm Media - IPF Media | -30.17 | 6.60 | (-49.76, -10.58) | -4.57 | 0.000 |
| Norm TLK - IPF Media | -22.20 | 6.60 | (-41.78, -2.61) | -3.37 | 0.018 |
| Norm H2O2 - IPF TLK | -24.13 | 6.60 | (-43.72, -4.54) | -3.66 | 0.008 |
| Norm Media - IPF TLK | -19.74 | 6.60 | (-39.33, -0.16) | -2.99 | 0.047 |
| Norm TLK - IPF TLK | -11.77 | 6.60 | (-31.36, 7.82) | -1.78 | 0.485 |
| Norm Media - Norm H2O2 | 4.39 | 6.60 | (-15.20, 23.98) | 0.67 | 0.985 |
| Norm TLK - Norm H2O2 | 12.36 | 6.60 | (-7.23, 31.95) | 1.87 | 0.430 |
| Norm TLK - Norm Media | 7.97 | 6.60 | (-11.61, 27.56) | 1.21 | 0.830 |

*Individual confidence level = 99.53%*

**Repeated Measures ANOVA**
**GST Analysis**
**Within Subjects Effects**

| | Sum of Squares | df | Mean Square | F | p |
|---|---|---|---|---|---|
| RM Factor 1 | 2.41 | 1 | 2.41 | 0.0309 | 0.865 |
| RM Factor 1 ✻ Disease | 8.04 | 1 | 8.04 | 0.1028 | 0.757 |
| RM Factor 1 ✻ Treatment | 20.81 | 1 | 20.81 | 0.2662 | 0.62 |
| RM Factor 1 ✻ Disease ✻ Treatment | 388.25 | 1 | 388.25 | 4.9661 | 0.056 |
| Residual | 625.45 | 8 | 78.18 | | |

Note. Type 3 Sums of Squares

**Between Subjects Effects**

| | Sum of Squares | df | Mean Square | F | p |
|---|---|---|---|---|---|
| Disease | 5051.5 | 1 | 5051.5 | 12.6609 | 0.007 |
| Treatment | 20.8 | 1 | 20.8 | 0.0522 | 0.825 |

| | | | | | |
|---|---|---|---|---|---|
| Disease ✻ Treatment | 388.3 | 1 | 388.3 | 0.9731 | 0.353 |
| Residual | 3191.9 | 8 | 399 | | |

Note. Type 3 Sums of Squares

## REFERENCES


1. Kim, H. J., Perlman, D. & Tomic, R. Natural history of idiopathic pulmonary fibrosis. *Respir. Med.* **109,** 661–670 (2015).
2. Ley, B. & Collard, H. R. Epidemiology of idiopathic pulmonary fibrosis. *Clin. Epidemiol.* **5,** 483–492 (2013).
3. Hutchinson, J. P., McKeever, T. M., Fogarty, A. W., Navaratnam, V. & Hubbard, R. B. Increasing Global Mortality from Idiopathic Pulmonary Fibrosis in the Twenty-First Century. *Ann. Am. Thorac. Soc.* **11,** 1176–1185 (2014).
4. King, T. E., Pardo, A. & Selman, M. Idiopathic pulmonary fibrosis. *The Lancet* **378,** 1949–1961 (2011).
5. Raghu, G. *et al.* An Official ATS/ERS/JRS/ALAT Clinical Practice Guideline: Treatment of Idiopathic Pulmonary Fibrosis: An Update of the 2011 Clinical Practice Guideline. *Am. J. Respir. Crit. Care Med.* **192,** E3–E19 (2015).
6. Richeldi, L. *et al.* Efficacy and Safety of Nintedanib in Idiopathic Pulmonary Fibrosis. *N. Engl. J. Med.* **370,** 2071–2082 (2014).
7. Kim, E. S. & Keating, G. M. Pirfenidone: A Review of Its Use in Idiopathic Pulmonary Fibrosis. *Drugs* **75,** 219–230 (2015).

8. Pollack, A. F.D.A. Approves First 2 Drugs for Treatment of a Fatal Lung Disease. *The New York Times* (2014).
9. Kliment, C. R. & Oury, T. D. Oxidative stress, extracellular matrix targets, and idiopathic pulmonary fibrosis. *Free Radic. Biol. Med.* **49,** 707–717 (2010).
10. Kurundkar, A. & Thannickal, V. J. Redox mechanisms in age-related lung fibrosis. *Redox Biol.* **9,** 67–76 (2016).
11. Cantin, A. M., Hubbard, R. C. & Crystal, R. G. Glutathione Deficiency in the Epithelial Lining Fluid of the Lower Respiratory Tract in Idiopathic Pulmonary Fibrosis. *Am. Rev. Respir. Dis.* **139,** 370–372 (1989).
12. Chapman, H. A. Epithelial-Mesenchymal Interactions in Pulmonary Fibrosis. *Annu. Rev. Physiol.* **73,** 413–435 (2011).
13. Fattman, C. L. Apoptosis in Pulmonary Fibrosis: Too Much or Not Enough? *Antioxid. Redox Signal.* **10,** 379–386 (2007).
14. Golan-Gerstl, R., Wallach-Dayan, S. B., Amir, G. & Breuer, R. Epithelial Cell Apoptosis by Fas Ligand-Positive Myofibroblasts in Lung Fibrosis. *Am. J. Respir. Cell Mol. Biol.* **36,** 270–5 (2007).
15. Selman, M. & Pardo, A. Alveolar Epithelial Cell Disintegrity and Subsequent Activation: A Key Process in Pulmonary Fibrosis. *Am. J. Respir. Crit. Care Med.* **186,** 119–121 (2012).
16. Safaeian, L., Abed, A. & Vaseghi, G. The role of Bcl-2 family proteins in pulmonary fibrosis. *Eur. J. Pharmacol.* **741,** 281–289 (2014).

17. King Jr, T. E., Pardo, A. & Selman, M. Idiopathic pulmonary fibrosis. *The Lancet* **378,** 1949–1961 (2011).
18. Hinz, B. *et al.* The Myofibroblast. *Am. J. Pathol.* **170,** 1807–1816 (2007).
19. Todd, N. W., Luzina, I. G. & Atamas, S. P. Molecular and cellular mechanisms of pulmonary fibrosis. *Fibrogenesis Tissue Repair* **5,** 11 (2012).
20. Bocchino, M. *et al.* Reactive Oxygen Species Are Required for Maintenance and Differentiation of Primary Lung Fibroblasts in Idiopathic Pulmonary Fibrosis. *PLoS ONE* **5,** e14003 (2010).
21. Cheresh, P., Kim, S.-J., Tulasiram, S. & Kamp, D. W. Oxidative stress and pulmonary fibrosis. *Biochim. Biophys. Acta BBA - Mol. Basis Dis.* **1832,** 1028–1040 (2013).
22. Waghray, M. *et al.* Hydrogen peroxide is a diffusible paracrine signal for the induction of epithelial cell death by activated myofibroblasts. *FASEB J.* **19,** 854–856 (2005).
23. Richter, K., Konzack, A., Pihlajaniemi, T., Heljasvaara, R. & Kietzmann, T. Redox-fibrosis: Impact of TGFβ1 on ROS generators, mediators and functional consequences. *Redox Biol.* **6,** 344–352 (2015).
24. Richter, K. & Kietzmann, T. Reactive oxygen species and fibrosis: further evidence of a significant liaison. *Cell Tissue Res.* **365,** 591–605 (2016).
25. Liu, R.-M. & Gaston Pravia, K. A. Oxidative stress and glutathione in TGF-β-mediated fibrogenesis. *Free Radic. Biol. Med.* **48,** 1 (2010).

26. Forman, H. J., Zhang, H. & Rinna, A. Glutathione: Overview of its protective roles, measurement, and biosynthesis. *Mol. Aspects Med.* **30,** 1–12 (2009).
27. Pubchem. glutathione | C10H17N3O6S - PubChem. Available at: https://pubchem.ncbi.nlm.nih.gov/compound/glutathione. (Accessed: 27th January 2017)
28. *Toxicology of Glutathione Transferases*. (Informa Healthcare, 2006).
29. Chakravarthi, S. & Bulleid, N. J. Glutathione Is Required to Regulate the Formation of Native Disulfide Bonds within Proteins Entering the Secretory Pathway. *J. Biol. Chem.* **279,** 39872–39879 (2004).
30. Jefferies, H. *et al.* Glutathione. *ANZ J. Surg.* **73,** 517–522 (2003).
31. Jefferies, H. *et al.* Glutathione. *ANZ J. Surg.* **73,** 517–522 (2003).
32. Strange, R. C., Spiteri, M. A., Ramachandran, S. & Fryer, A. A. Glutathione-S-transferase family of enzymes. *Mutat. Res. Mol. Mech. Mutagen.* **482,** 21–26 (2001).
33. Balendiran, G. K., Dabur, R. & Fraser, D. The role of glutathione in cancer. *Cell Biochem. Funct.* **22,** 343–352 (2004).
34. Guengerich, F. P. Common and Uncommon Cytochrome P450 Reactions Related to Metabolism and Chemical Toxicity. *Chem. Res. Toxicol.* **14,** 611–650 (2001).
35. Testa, B. & Krämer, S. D. The Biochemistry of Drug Metabolism – An Introduction. *Chem. Biodivers.* **3,** 1053–1101 (2006).
36. Josephy, P. D., Guengerich, F. P. & Miners, J. O. "Phase I and Phase II" Drug Metabolism: Terminology that we Should Phase Out? *Drug Metab. Rev.* **37,** 575–580 (2005).

37. Rushmore, T. H. & Pickett, C. B. Glutathione S-transferases, structure, regulation, and therapeutic implications. *J. Biol. Chem.* **268,** 11475–11478 (1993).

38. Mahajan, S. & Atkins, W. M. The chemistry and biology of inhibitors and pro-drugs targeted to glutathione S-transferases. *Cell. Mol. Life Sci. CMLS* **62,** 1221–1233 (2005).

39. Zhou, S. *et al.* Functional Interaction of Glutathione S-transferase pi and Peroxiredoxin 6 in Intact Cells. *Int. J. Biochem. Cell Biol.* **45,** 401–407 (2013).

40. Rhee, S. G. Overview on Peroxiredoxin. *Mol. Cells* **39,** 1–5 (2016).

41. Manevich, Y., Feinstein, S. I. & Fisher, A. B. Activation of the antioxidant enzyme 1-CYS peroxiredoxin requires glutathionylation mediated by heterodimerization with πGST. *Proc. Natl. Acad. Sci. U. S. A.* **101,** 3780–3785 (2004).

42. Watson, W. H., Ritzenthaler, J. D. & Roman, J. Lung extracellular matrix and redox regulation. *Redox Biol.* **8,** 305–315 (2016).

43. Anathy, V. *et al.* Redox-Based Regulation of Apoptosis: S-Glutathionylation As a Regulatory Mechanism to Control Cell Death. *Antioxid. Redox Signal.* **16,** 496–505 (2012).

44. Laborde, E. Glutathione transferases as mediators of signaling pathways involved in cell proliferation and cell death. *Cell Death Differ.* **17,** 1373–1380 (2010).

45. Board, P. G. & Menon, D. Glutathione transferases, regulators of cellular metabolism and physiology. *Biochim. Biophys. Acta BBA - Gen. Subj.* **1830,** 3267–3288 (2013).

46. Anathy, V. *et al.* Oxidative Processing of Latent Fas in the Endoplasmic Reticulum Controls the Strength of Apoptosis. *Mol. Cell. Biol.* **32,** 3464–3478 (2012).

47. Janssen-Heininger, Y. M. W. *et al.* Regulation of apoptosis through cysteine oxidation: implications for fibrotic lung disease. *Ann. N. Y. Acad. Sci.* **1203,** 23–28 (2010).

48. Loomis-King, H., Flaherty, K. R. & Moore, B. B. Pathogenesis, current treatments and future directions for idiopathic pulmonary fibrosis. *Curr. Opin. Pharmacol.* **13,** 377–385 (2013).

49. Hagimoto, N. *et al.* Induction of Apoptosis and Pulmonary Fibrosis in Mice in Response to Ligation of Fas Antigen. *Am. J. Respir. Cell Mol. Biol.* **17,** 272–278 (1997).

50. Nguyen, T., Nioi, P. & Pickett, C. B. The Nrf2-Antioxidant Response Element Signaling Pathway and Its Activation by Oxidative Stress. *J. Biol. Chem.* **284,** 13291–13295 (2009).

51. Zhao, H., Eguchi, S., Alam, A. & Ma, D. The role of nuclear factor-erythroid 2 related factor 2 (Nrf-2) in the protection against lung injury. *Am. J. Physiol. - Lung Cell. Mol. Physiol.* **312,** L155–L162 (2017).

52. Ruscoe, J. E. *et al.* Pharmacologic or Genetic Manipulation of Glutathione S-Transferase P1–1 (GSTπ) Influences Cell Proliferation Pathways. *J. Pharmacol. Exp. Ther.* **298,** 339–345 (2001).

53. Jones, J. T. *et al.* Glutathione S-transferase pi modulates NF-κB activation and pro-inflammatory responses in lung epithelial cells. *Redox Biol.* **8,** 375–382 (2016).

54. McMillan, D. H. *et al.* Attenuation of lung fibrosis in mice with a clinically relevant inhibitor of glutathione-S-transferase π. *JCI Insight* **1,** (2016).

55. Raza, A. *et al.* A phase 2 randomized multicenter study of 2 extended dosing schedules of oral ezatiostat in low to intermediate-1 risk myelodysplastic syndrome. *Cancer* **118,** 2138–2147 (2012).

56. Raza, A. *et al.* Phase 1 multicenter dose-escalation study of ezatiostat hydrochloride (TLK199 tablets), a novel glutathione analog prodrug, in patients with myelodysplastic syndrome. *Blood* **113,** 6533–6540 (2009).

57. Emblom-Callahan, M. C. *et al.* Genomic phenotype of non-cultured pulmonary fibroblasts in idiopathic pulmonary fibrosis. *Genomics* **96,** 134–145 (2010).

58. Pfaffl, M. W. A new mathematical model for relative quantification in real-time RT–PCR. *Nucleic Acids Res.* **29,** e45 (2001).

59. Hayes, J. D., Flanagan, J. U. & Jowsey, I. R. Glutathione Transferases. *Annu. Rev. Pharmacol. Toxicol.* **45,** 51–88 (2005).

60. Charles G. B. Caraguel, Henrik Stryhn, Nellie Gagné, Ian R. Dohoo & K. Larry Hammell. Selection of a Cutoff Value for Real-Time Polymerase Chain Reaction Results to Fit a Diagnostic Purpose: Analytical and Epidemiologic Approaches. *J. Vet. Diagn. Invest.* **23,** 2–15 (2011).

61. Balogh, L. M. & Atkins, W. M. Interactions of glutathione transferases with 4-hydroxynonenal. *Drug Metab. Rev.* **43,** 165–178 (2011).

62. Halliwell, B. & Chirico, S. *..1,n J C/in Nutr 1993:57(suppl):7 15S-25S. Printed in USA. © 1993 American Society for Clinical Nutrition 715S Lipid peroxidation: its mechanism, measurement, and significanc&3*.

63. Balogh, L. M. *et al.* Substrate Specificity Combined with Stereopromiscuity in Glutathione Transferase A4-4-Dependent Metabolism of 4-Hydroxynonenal. *Biochemistry (Mosc.)* **49,** 1541–1548 (2010).

64. Raza, H. & John, A. 4-Hydroxynonenal induces mitochondrial oxidative stress, apoptosis and expression of glutathione S-transferase A4-4 and cytochrome P450 2E1 in PC12 cells. *Toxicol. Appl. Pharmacol.* **216,** 309–318 (2006).

65. Hou, J. *et al.* TNF-α-induced NF-κB activation promotes myofibroblast differentiation of LR-MSCs and exacerbates bleomycin-induced pulmonary fibrosis. *J. Cell. Physiol.* **233,** 2409–2419 (2018).

66. Habiel, D. M. & Hogaboam, C. Heterogeneity in fibroblast proliferation and survival in idiopathic pulmonary fibrosis. *Front. Pharmacol.* **5,** (2014).

67. Tew, K. D. & Townsend, D. M. Regulatory functions of glutathione S-transferase P1-1 unrelated to detoxification. *Drug Metab. Rev.* **43,** 179–193 (2011).

68. Morel, F. *et al.* Gene and protein characterization of the human glutathione S-transferase kappa and evidence for a peroxisomal localization. *J. Biol. Chem.* **279,** 16246–16253 (2004).

69. Friling, R. S., Bensimon, A., Tichauer, Y. & Daniel, V. Xenobiotic-inducible expression of murine glutathione S-transferase Ya subunit gene is controlled by an electrophile-responsive element. *Proc. Natl. Acad. Sci.* **87,** 6258–6262 (1990).

70. Lushchak, V. I. Glutathione Homeostasis and Functions: Potential Targets for Medical Interventions. *Journal of Amino Acids* (2012). doi:10.1155/2012/736837

71. Dhakshinamoorthy, S. & Jaiswal, A. K. c-Maf negatively regulates ARE-mediated detoxifying enzyme genes expression and anti-oxidant induction. *Oncogene* **21,** 1205642 (2002).

72. Kim, Y.-C. *et al.* Hemin-induced Activation of the Thioredoxin Gene by Nrf2 A DIFFERENTIAL REGULATION OF THE ANTIOXIDANT RESPONSIVE ELEMENT BY A SWITCH OF ITS BINDING FACTORS. *J. Biol. Chem.* **276,** 18399–18406 (2001).

73. Zucker, S. N. *et al.* Nrf2 amplifies oxidative stress via induction of Klf9. *Mol. Cell* **53,** 916–928 (2014).

74. Mazur, W. *et al.* Cell-specific elevation of NRF2 and sulfiredoxin-1 as markers of oxidative stress in the lungs of idiopathic pulmonary fibrosis and non-specific interstitial pneumonia. *APMIS* **118,** 703–712 (2010).

75. Swamy, S. M., Rajasekaran, N. S. & Thannickal, V. J. Nuclear Factor–Erythroid-2–Related Factor 2 in Aging and Lung Fibrosis. *Am. J. Pathol.* **186,** 1712–1723 (2016).

## BIOGRAPHY

Eileen Liberti graduated from Jamesville DeWitt High School, Fayetteville, New York, in 1980. She received her Bachelor of Science from Saint Bonaventure University in 1984. She was employed as a laboratory technician for Boston University Medical and as a pharmaceutical sales representative. Mrs. Liberti is currently a teacher at Paul VI Catholic High School in Fairfax, Virginia.